NTNU

Norwegian University of
Science and Technology

A Slim Wind Turbine Concept with Low Frequency AC Connection

Andreas Nyhagen Hole

Master of Energy and Environmental Engineering
Submission date: June 2016
Supervisor: Kjetil Uhlen, ELKRAFT
Co-supervisor: Sverre Skalleberg Gjerde, Statkraft AS

Norwegian University of Science and Technology
Department of Electric Power Engineering

Problem Description

As the offshore wind farms are getting larger, and at the same time, the distance to shore is increasing, upcoming projects may be outside the reach of traditional HVAC-cables used as export cables. The common view is then to make use of VSC-HVDC. However, this introduces several new challenges such as cost and reliability. As an alternative, low frequency AC (LFAC) has been proposed. Although promising, several technology gaps and uncertainties need to be investigated before the LFAC can be implemented in a wind farm. An interesting option with this topology is to make use of a slim wind turbine concept excluding the converter. The idea is then to control the entire the entire wind farm with a common variable frequency from the onshore converter station.

The thesis should develop a model of the proposed system and implement a suitable control strategy. The challenges that the proposed system faces should be highlighted. Based on the results from the simulations and the challenges found, some measures should be done in order to overcome these. Measures to reduce losses in the system should also be approached. The model and the results will lay the foundation for further research on the feasibility of the proposed system.

Abstract

This thesis aims to investigate the feasibility of using a slim wind turbine concept together with a low frequency alternating current (LFAC) transmission system in an offshore wind farm system. By a slim wind turbine concept, it is referred to a wind turbine where the converter is excluded. The idea is to use large direct drive PMSGs that will output a low frequency AC directly. The proposed system will have all wind turbines operating synchronously where an onshore converter station will be able to control the whole wind farm. The work has focused on developing a model in MATLAB Simulink, implementing a suitable control system and study different ways of minimizing losses. The challenges that the proposed system faces are highlighted and measures to minimize the reactive flow in the system has been tested.

The proposed system is illustrated in Figure 1. The wind turbine is based on the 10 MW NOWITECH reference turbine. Aggregated models are utilized in order to save computational time. An average model is used to model the onshore converter where only the generator side converter is included. The development of the model is explained in the thesis and further improvements are suggested.

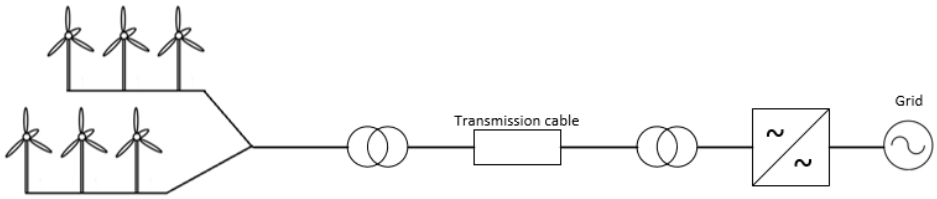

Figure 1: The proposed system studied in this thesis.

The control system implemented in the frequency converter is based on the power signal feedback control. The difference between those will be that the converter controls the frequency, and hence the speed, based on power measurements. Obtaining an optimal frequency versus power curve as a reference for the control system is proved to be difficult as the losses in the system varies with the system frequency. The results show the clear disadvantage of having all turbines operate synchronously when they are exposed to different wind speeds as this results in lost power production compared to a system with independently speed control.

Varying the system frequency will have an impact on the components in the system. Lowering the frequency results in less reactive power generated in the cable while the the shunt reactors will demand more reactive power. The results also showed that the generators starts to draw a serious amount of reactive power in order to maintain the active power production at rated voltage level. This proves the necessity of FACTS-devices and hence an active compensation was tested. Due

to the simplifications made this resulted in severe oscillations in the system. The oscillations were proven to have a frequency equal to the system frequency which could prove this system to be infeasible. Further research and testing of this feature should be carried out.

Operation at a lower transmission voltage level was also tested during a wind farm power production of 0.6 pu. By lowering the voltage, the charging currents will be reduced and hence the losses will be reduced. The results showed that by lowering the voltage level to 0.8 pu the losses were reduced by 9.29 % when no other changes in the model were done. Lowering the losses is an important economic factor, but it will also increase the feasible operation range, allowing the system to operate under even lower wind speeds.

Samandrag

Denne avhandlinga siktar på å undersøkje mogelegheita av å bruke eit forenkla vind turbin konsept i lag med eit lav frekvent vekselstraum (LFAC) overførings system innan ein offshore vindpark. Med ein forenkla turbin er det meint ein turbin der frekvensomformaren er fjerna. Ideen går ut på å bruke store direkte drivne permanent magnet synkron generatorar (PMSGs) som vil generere ein LFAC direkte. I det føreslåtte systemet vil alle vindturbinane operere synkront og ein vil ha ein omformarstasjon på land som vil kunne styre heile vindparken. Arbeidet har fokusert på å utvikle ein modell i MATLAB Simulink, implementere eit passande kontrollsystem og studere ulike måtar å minimalisere tapa i systemet. Utfordringane til systemet er blitt framheva og metodar for å minimalisere reaktiv effektflyt i systemet har blitt testa.

Det føreslåtte systemet er illustrert i Figur 2. Vindturbinane er basert på NOWITECH sin 10 MW referanse turbin. Ein samla modell for fleire turbinar er brukt for å spare bereknings tid. Ein gjennomsnittsmodell blir brukt for å modellere den landbaserte omformarstasjonen der kunn generator side omformaren er inkludert. Utviklinga av modellen er forklart i avhandlinga og forslag til forbetringar er føreslått.

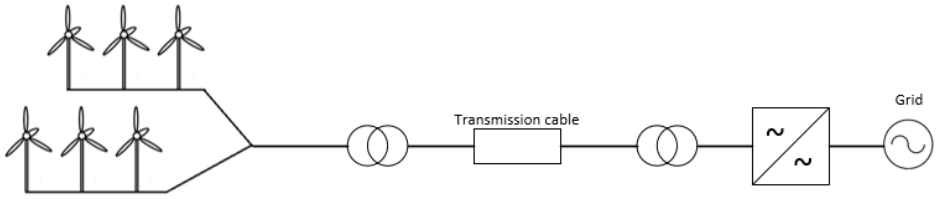

Figur 2: Det føreslåtte systemet studert i denne avhandlinga.

Kontrollsystemet som er implementert i omformaren er basert på tilbakekopla effektsignal kontroll. Forskjellen mellom dei er at omformaren no kontrollerer frekvensen i systemet, og dermed også rotasjonshastigheten til turbinane, basert på effektmålingar. Oppbygging av ein optimal frekvens versus effekt kurve som ein referanse for reguleringssystemet har vist seg å vere vanskelig ettersom tapa i systemet varierer med frekvensen. Resultata viser tydelig den negative sida av at alle turbinane opererer synkront når dei blir utsatt for ulik vindhastighet. Det fører til at ikkje alle turbinane kan operere på optimalt produksjonsnivå og ein vil dermed tape effekt samanlikna med eit system der ein kan styre rotasjonshastigheten uavhengig av dei andre turbinane.

Ein varierande system frekvens vil påverke komponentane i systemet og deira eigenskapar. Redusering av frekvensen fører til mindre reaktive effekt generert i kabelen medan reaktoren vil krevje meir reaktiv effekt. Resultata viser også

at generatorane vil starte å dra store mengder reaktiv effekt for å oppretthalde aktiv effekt produksjon ved merkespenning når frekvensen reduserast. Dette viser behovet for FACTS komponentar som aktivt kan styre reaktiv effekt kompensering når det er behov for det og dette blei derfor testa. Som følgje av forenklingane resulterte dette i store svingingar i systemet. Svingingane blei funnet til å ha ein frekvens lik system frekvensen, noko som kan vere ein indikator på at dette systemet ikkje lar seg gjere. Vidare forsking og testing av dette bør gjennomførast.

Drift ved ein lågare overføringsspenning blei også testa for ein situasjon der vindparken har ein kraftproduksjon på 0.6 pu. Ved å senke spenninga vil ein redusere ladningsstraumar og dermed også redusere tapa i overføringa. Resultata viste at ved å senke spenninga til 0.8 pu reduserte ein tapa med 9.29 %. Å redusere tapa er ein viktig økonomisk faktor, men også fordi det vil føre til at vindparken kan operere under endå lågare vindhastigheter.

Preface

This thesis summarizes the work I've been doing in my 10th and last semester as a master student at the Department of Electrical Power Engineering at Norwegian University of Science and Technology (NTNU). The master thesis is a further extension of the work done in the specialization project in my 9th semester where I was attending as a guest student at the Technical University of Denmark (DTU). The thesis was initiated by Statkraft AS and serve to investigate a possible solution for offshore wind farms.

This last semester has been really valuable for me. My thesis work has been challenging in many ways and it has prepared me for new challenges in my future career. I'm grateful for all the help, support and encouragement I've had from my surroundings and I want to thank those who have contributed to the work.

First I would like to thank my supervisor, Professor Kjetil Uhlen, for his valuable supervision and guidance. I would also express my sincerely gratefulness for helping me make the exchange to DTU possible by setting me in contact with the technical environment there.

Then I also express thankfulness to Karstein Brekke, from Statkraft AS, whom took upon himself to be my contact person the last month of my work, helping me set some deadlines and giving me tips for writing the report.

Last I would like to thank Dr. Sverre Skalleberg Gjerde, my supervisor and contact person in Statkraft AS during the last year. He initiated the project and has been a great resource through the master year. He has truly taken his time to answer my question and I'm grateful of having had him as my supervisor.

Trondheim 10.06.2016

Andreas Nyhagen Hole

Contents

List of Figures

List of Tables

Abbreviations

AC Alternating Current

DFIG Doubly-Fed Induction Generator

emf Electromotive Force

FACTS Flexible Alternating Current Transmission System

GSC Generator Side Converter

HCS Hill Climb Search

HVAC High Voltage Alternating Current

HVDC High Voltage Direct Current

LCC Line Commutated Converter

LFAC Low Frequency Alternating Current

MMC Modular Multilevel Converter

MPP Maximim Power Point

MPPT Maximum Power Point Tracking

OT Optimal Torque

PMSG Permanent Magnet Synchronous Generator

PSF Power Signal Feedback

pu Per-Unit

PWM Pulse Width Modulation

SSC System Side Converter

SVM Space Vector Modulation

TSR Tip Speed Ratio

VSC Voltage Source Converter

WPGS Wind Power Generation System

Chapter 1

Introduction

1.1 Background and Motivation

The constant increase of the world population creates a huge demand for energy in the future. Combined with the necessity of reducing the CO_2-emissions the use of renewable energy sources will be even more important for each year that goes by. As most of the sites with hydro power potential already have been used, the industry look towards the wind power potential located offshore. Despite the currently large costs associated with offshore wind power it has recently gained a lot more interest due to the above mentioned challenge.

The wind power industry, both onshore and offshore, has had a significant growth the past years. In Europe the annual wind power installations have increased steadily from 3.2 GW in 2000 to 11.8 GW in 2014 [1]. A total of 128.8 GW is now installed in the European Union, whereas only just over 8 GW is offshore wind power. Given the right support, the Wind Energy Technology Platform predicts that up to 34 % of the Europe's electricity demand can be provided by wind energy in 2030 [2]. This require a long-term strategic approach in terms of technology and policy research. Europe has enormous offshore wind power potential because of the large available areas and the high mean annual wind speed. Exploitation of this resource will be a key-factor for reaching this amount of wind power. The structure used for offshore wind turbines comes with new challenges due to the water depth and thereby increased costs. Among other things, it is therefore of great interest to have as large wind turbines as possible. Today, the largest wind turbine is the Vestas V-164 8 MW, which is placed onshore in Denmark. Along with other large wind turbines as Enercons E-126 7.5 MW this proves that a large scale wind turbine is possible.

As the offshore wind farms are getting larger several other challenges appears. One of them is the transmission of power to shore due to increased distance and

amount of power being transmitted. Upcoming project may therefore be outside the reach of standard AC cables, as the capacitive charging current limits the power being transmitted through the cable. For distances over 90 km it would therefore be cheaper to use a high voltage direct current (HVDC) system for connecting a 100 MW wind farm [3]. The use of HVDC system introduces a new challenge like reliability. Therefore, as an alternative, low frequency AC (LFAC) system has been proposed. Although promising results, several technology gaps and uncertainties needs to be investigated before LFAC transmission can be implemented as the transmission system for a wind farm. A feasibility study in use of LFAC for offshore wind farms with respect to wind turbine implications was made by Statkraft [4]. An interesting option, that was suggested for further study in the report, was to strip down the equipment in each turbine, and develop a slimmed turbine. By using large direct-drive permanent magnet synchronous generators (PMSG) that will output this low frequency AC directly, there is no need for a frequency converter offshore. An option is to have all the wind turbines at the offshore wind farm operating synchronously at the same speed. The frequency converter is then placed onshore, controlling the entire wind farm with a common variable frequency. By the term "slim turbine concept" one will in this thesis refer to a wind turbine with no converter. The concept of stripping the turbines could have an economic advantage. Combining it with the use of LFAC transmission, which has proved to be a cost effective solution, and which also increase the possible transmission distance, could make it a competitive solution to the current wind farm systems [5]. No such configuration exist today, and it is not found any previous work on using this proposed slim turbine concept. It is however found some research on the use of LFAC transmission and how it will impact other components in the system [4] [6] [7].

1.2 Objectives

This thesis aims to investigate the feasibility of using a slimmed turbine concept together with LFAC transmission as an alternative to offshore wind farm systems. The work has focused on developing a model in MATLAB Simulink that can be used for further studies, implementing a suitable control system and study different ways of minimizing losses. The challenges that the proposed system faces are highlighted and measures to minimize the reactive power flow in the system has been tested.

1.3 Relation to Specialization Project

This thesis is an extension of the work that the author did as a part of the specialization project during his stay at the Technical University of Denmark (DTU) in the fall of 2015. The report was titled "Low Frequency AC - Slim Turbine

Concept". The work done in this thesis aims to further investigate some of the challenges found in this work. The model used in this thesis is a development of the model made during the project. In order to form a more complete and independent text some of the material from the specialization project has therefore been used in this thesis.

1.4 Structure of the Thesis

In Chapter 2 a brief presentation of the wind turbine technology and the different transmission systems is given. The impact of introducing a lower frequency to the components in the system is also presented. Chapter 3 presents the background theory for the work done in this thesis. The voltage source converter (VSC), different techniques for maximum power point tracking (MPPT) and control of the PMSG are some of the topics that are addressed. Chapter 4 presents the model made in MATLAB Simulink SimPowerSystems, which may also serve as a base for further study within the proposed system. In Chapter 5 the control concept used in this thesis and the modelling of it is presented. The results are presented in Chapter 6 together with the different cases that were looked into and the discussion of the results.

Chapter 2

Wind Turbines and Transmission Systems

2.1 Wind Turbine Technology

Today, there are several wind turbines on the market with different types of generators and power electronics [8]. Wind turbines are classified by their ability to control speed and by the type of power control used. Wind turbines operates either with a fixed speed or a variable speed. Fixed speed wind turbines are typically equipped with an induction generator that is directly connected to the grid. They also comes with a capacitor bank for reducing reactive power compensation and a soft starter in order to reduce transient current during connection of the generator to the grid. These turbines are designed to achieve maximum efficiency at only one particular wind speed. The advantage of these turbines are that they are simple, cheap, robust and reliable. However, the disadvantages of an uncontrollable reactive power consumption, mechanical stress and limited power quality control makes it less attractive.

The variable speed wind turbines has become the dominant type among the installed wind turbines the last decade [8]. They are usually referred to as Type C and Type D and can be seen in Figure 2.1. Most commonly they use an induction or synchronous generator which is connected to the grid through a power converter. These turbines are designed to achieve maximum efficiency over a wide range of wind speeds. Here the rotational speed, ω, of the wind turbine can be controlled to a suitable speed according to the wind speed, V_w. The variations in wind will therefore be absorbed by a change in the generator speed making it able to keep the generator torque rather constant. The advantage of this type is an improved power quality, increased energy capture and a reduced mechanical stress on the wind turbine. The disadvantage is that the use of power electronics increase the cost of

equipment significantly making it a very expensive choice. Another disadvantage are the extra losses that occurs in the power electronics.

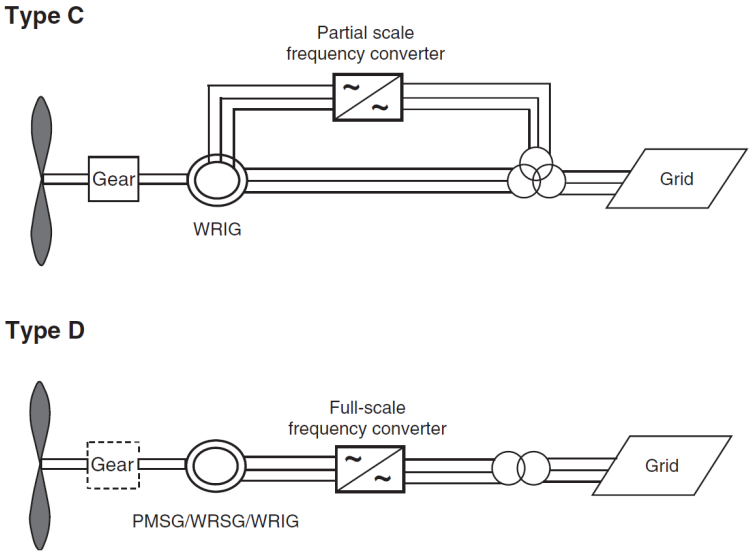

Figure 2.1: Doubly fed induction generator (DFIG) wind turbine (Type C) and a full converter wind turbine (Type D) [8].

All wind turbines are designed with some sort of power control in order to avoid damage to the wind turbine [8]. There are three different ways of controlling the aerodynamic forces on the turbine rotor. The first one is called stall control, or passive control, and is the cheapest, most robust and simplest one. The blades, which are bolted onto the hub at a fixed angle, is designed so that the rotor stalls, or lose power, when the wind speed exceeds a certain level. The second type of control is the pitch control, also called active control, where the blades are no longer bolted on the hub at a fixed angle. Here the blades can be turned out or into the wind in order to decrease or increase the power output. The third option is the active stall control where the stall of the blade is actively controlled by pitching the blades. This option achieves a lot smoother limited power with no high power fluctuations in addition to being able to compensate for air density variations.

2.2 Transmission Technology

Offshore installations requires submarine cables for power transmission to shore. Today, most of the wind farms are connected through a high voltage alternating current (HVAC) network with a frequency of 50 or 60 Hz [9]. However, due to the increased distance to shore and the increased power transmitted HVDC network has

been considered as a better alternative. Recently, a relative new concept that might challenge the HVDC have become more attractive, namely the LFAC network. Figure 2.2 shows the different layouts for the transmission systems. In this section the different technologies will be briefly presented in terms of their advantages and disadvantages.

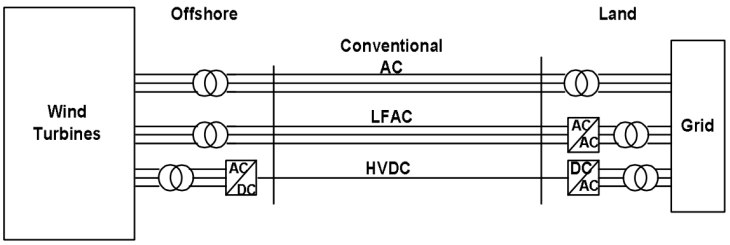

Figure 2.2: The layouts of the offshore wind farms transmission systems [5].

2.2.1 High Voltage Alternating Current

The HVAC transmission system is a well-known technology and are currently the preferred solution for distances up to around 100 km [8]. HVAC transmission is advantageous because it is relatively simple to design the protection systems and to change voltage levels using transformers [10]. However, the high capacitance of submarine AC power cables leads to substantial charging currents which reduces the active power transmission capacity and limits the transmission distance. In order to improve the transmission capacity and efficiency reactive power compensation, like shunt reactors, can be installed. The shunt reactors can be placed in either end of the cable, or both ends. The feasible transmission length will be dependent on the additional costs related to this.

2.2.2 High Voltage Direct Current

When the transmission distance exceeds a certain length the use of HVAC becomes unfeasible due to the high charging currents and the cost related to compensation. Then HVDC becomes the preferred technology. The main advantage of using HVDC transmission is that it impose no transmission distance limit as a result of the absence of charging currents in the cable. There are two technical options for HVDC systems, depending on the types of power-electronic devices used, line commutated converter (LCC) based HVDC and voltage source converter (VSC) based HVDC technology [8]. LCC-HVDC systems are capable of transmitting power up to 1 GW with high reliability [10]. However, this technology requires large

converter stations both onshore and offshore. It also requires auxiliary equipment, such as AC filters, capacitor banks or static synchronous compensators, because LCC systems draw reactive power from the grid. The auxiliary service shall provide a strong offshore AC system in order for the LCC to operate during periods with very little wind. In contrary, VSC systems does not require a strong offshore or onshore AC system, it can actually start up against a nonload AC network. The VSC system are also capable of independently regulate active and reactive power exchanged with the onshore grid and the offshore AC collection grid. The drawbacks of this topology is the reduced efficiency and the cost of the converters. Both power levels and reliability are lower than for the LCC-HVDC system. The power ratings are typically around 200-600 MW per converter [8].

2.2.3 Low Frequancy Alternating Current

To deal with the shortcomings of the HVAC system and at the same time avoid the costly HVDC system, the use of LFAC has been proposed. LFAC is based on the regular HVAC system, but with the use of a lower frequency as the name indicates [4]. The turbines could output the low frequency AC directly from the generator or through a frequency converter. By a lower frequency one typically refers to frequency at 20 Hz or 16 $\frac{2}{3}$ Hz, in other words, a third of the normal grid frequency.

By using LFAC there is no need of expensive offshore power converter stations. However, it is necessary to have a onshore converter station in order to transform the frequency to the normal grid frequency. By using a lower frequency the charging currents produced in the cable is significantly reduced. The losses due to skin effect are minimised to a negligible level. As a result of this the transmission capacity and the length of the cables will be increased. Introducing a lower frequency to the transmission system will have an effect on some of the other components in the system and it is therefore also necessary to investigate these effects as well.

Cable

Submarine cables can be used without any modification. There is no difference in design between cables with a frequency of 50 Hz or 16 $\frac{2}{3}$ Hz [6]. However, its impact on the electrical properties in the cable is quite different and also the main motivation of using a lower frequency. The capacitive and inductive reactances in the cable are given by:

$$\begin{aligned} X_C &= -\frac{1}{2\pi f C} \\ X_L &= 2\pi f L \end{aligned} \tag{2.1}$$

where f is the frequency and C and L are the capacitance and inductance of the

cable per unit length. From this equation it can be observed that a decrease in frequency will increase the capacitive reactance and decrease the inductive reactance. An increase in the capactive reactance will reduce the capacitive charging currents in the cable and hence increase the feasible distance of active power transmission. The advantage of a decreased inductive reactance can be explained by looking at the following simplified equation for active power being transmitted through cables or lines [5]:

$$P = \frac{V_S V_R}{X_L} sin\delta \tag{2.2}$$

Where V_S and V_R are the sending end and receiving end voltages respectively, X_L is the line reactance and δ is the transmitting angle. From Equation 2.2 it can be observed that the active power being transmitted will increase as a result of a reduced inductive reactance. The LFAC system is not only able to increase the transmitting power, but it will also improve the voltage stability, as illustrated in equation 2.3 given the same amount of reactive power transmitted.

$$\Delta V\% = \frac{QX_L}{V^2} \times 100 \tag{2.3}$$

ΔV is the voltage drop over the cable, V is the nominal voltage and Q is the reactive power flow of the cable. As a result of the lower frequency and thereby decreased impedance, the voltage drop over the cable is proportionally reduced.

Transformers

The most affected components are the transformers. Lowering the frequency implies an increase in the size of the transformer, which can be shown in Equation 2.4 [7].

$$E = 4.44 \cdot fNBA \tag{2.4}$$

Where E is the induced electromotive force (emf) of the winding, f is the frequency, N is the number of turns in the winding, B is the peak magnet flux density and A is the cross-sectional area of the core. When the frequency is lowered the only variables that can be changed in order to maintain the same induced emf of the winding is the number of turns and the cross-section area, both leading to a weight and size increase of the transformer. The increase is further studied in [7], where it is found to be almost twice the size. The severe increase of the transformer will make it more expensive and it may lead to the necessity of redesigning the whole nacelle considering space issue. On the other hand, the use of low frequency reduces the windings and core losses in the transformer compared to the 50 Hz transformer [11].

Switchgear

SF6 circuit breakers for 16 $\frac{2}{3}$ Hz have been in commercial use for several years in the Swiss and German railway systems. However, compared to a power transmission grid the voltages levels for the railway system is small. The circuit breakers must therefore be further developed and modified for operations at a higher voltage level. On the other hand, the short circuit level within offshore grids are much lower than in the railway systems which makes short-circuit interruption easier [6].

Chapter 3

Background Theory

3.1 Voltage Source Converters

"Power electronic converters are a fundamental component in electrical energy conversion. They have several applications within the field of renewable energy because they can improve the efficiencies and power quality" [12].

3.1.1 Principles of Operation

VSCs are bidirectional ac/dc power converters which uses fully controllable switching semiconductor devices [13]. VSCs can be both single phase or three-phase VSCs. The most common type is the three-phase VSC and hence the acronym VSC is commonly used as reference for a three-phase VSC. The operating principles of VSC can easily be understood by tracking its topology back to the switch mode DC-DC step-down (buck) converter and step-up (boost) converter.

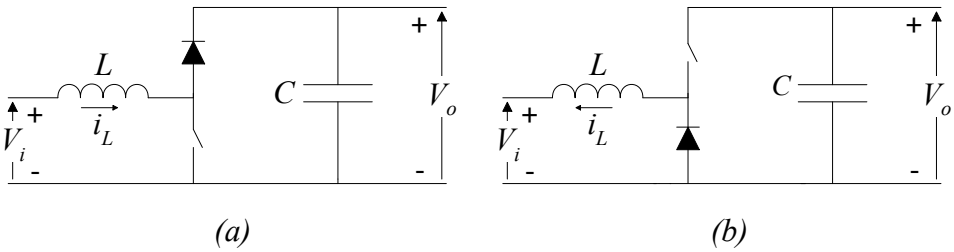

Figure 3.1: (a) Step-up (boost) and (b) step-down (buck) converters.

Note that in Figure 3.1 the step-down converter is inverted in order to compare its structure with the step-up converter. Hence the step-up and step-down converter convey power in opposite directions. The symbols L and C in Figure 3.1 refer to

the current smoothing inductive filter and the voltage smoothing capacitive filter respectively.

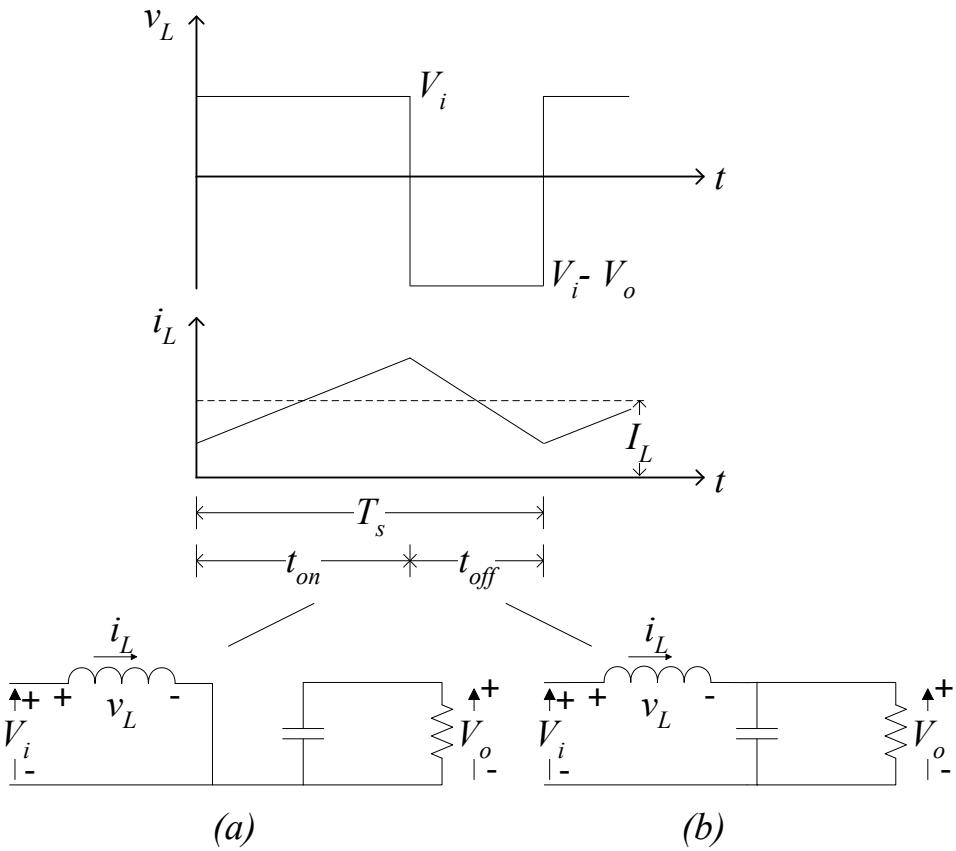

Figure 3.2: Continuous-conduction mode for a step up converter: (a) switch on; (b) switch off [14].

The working principle of the step-up converter can be explained by looking at the inductor voltage during continuous-conduction mode [14]. When the switch is on, the diode is reversed biased and thereby isolating the output stage. When the switch is off, the output stage will receive energy from both the inductor and the input. The time integral of the inductor voltage over one time period must be equal to zero under steady state. As seen from Figure 3.2 the integral can be written as

$$V_i t_{on} + (V_i - V_o) t_{off} = 0 \tag{3.1}$$

Dividing both sides by T_s and rearranging terms the relation between the voltages becomes

$$V_i = (1 - D)V_o \tag{3.2}$$

Applying the same procedure for the step-down converter gives

$$(V_i - V_o)t_{on} + V_i t_{off} = 0 \tag{3.3}$$

which results in

$$V_i = DV_o \tag{3.4}$$

The time period T_s is defined by the switching frequency, f_s, and the duty ratio, D, of a switch is defined as the ratio of its on-state time during one time period.

$$T_s = \frac{1}{f_s} \tag{3.5}$$

$$D = \frac{t_{on}}{T_s} \tag{3.6}$$

As the step-up converter and the step-down converter transfer power in opposite directions it is possible to combine them in order to make a bidirectional DC-DC converter [13]. The bidirectional switch mode converter is shown in Figure 3.3 and is commonly known as a half-bridge, excluding the capacitor. When the current in the inductor flows from left to the right, only the step-up converter part will be active while the step-down converter inactive. Similarly when the current flows in the opposite direction, the step-down converter will be active and the step-up converter will be the one whose inactive. Under normal operation of the bidirectional DC-DC converter the voltage on the left side, V_i, has to be less than the voltage on the right side, V_o. This constraint implies that the voltage input can be an AC voltage with an amplitude less than the output voltage, V_o. In other words it can work as a switch-mode bidirectional AC-DC converter.

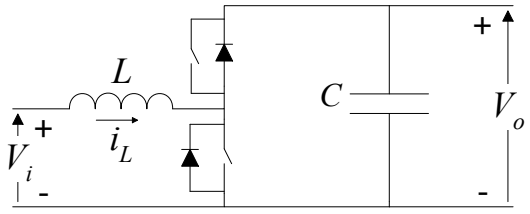

Figure 3.3: Bidirectional switch mode converter.

The most commonly used converter topology is the full-bridge converter. This is made by connecting two half-bridge switch mode converters to a common DC-bus as shown in Figure 3.4.

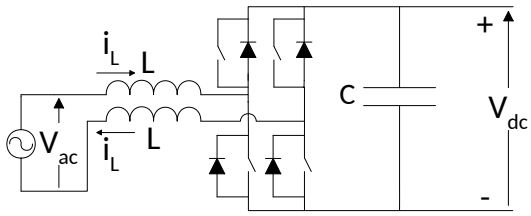

Figure 3.4: Full-bridge switch mode converter.

By adding another half-bridge one ends up with a three-phase switch mode converter usually referred to as a VSC [13]. In a VSC each half-bridge is connected to different phases in a three-phase system. Figure 3.5 shows the diagram of a two-level VSC, where v_a, v_b and v_c represent the phase voltages while P and N represent the points for positive and negative potential of the DC-link. From Figure 3.5 it can be seen that the line current in phase A runs through either T_{pa}, T_{na} or their respective diodes. By using Kirchoff's voltage law one get that $v_{aN} = v_a - v_N$ will be v_{dc} or 0, depending on which switch or diode is conducting. The phase voltages will therefore be of a square-wave form. However, as the switching frequency can be a lot higher than the fundamental frequency, good approximations to sinusoidal waves can be achieved.

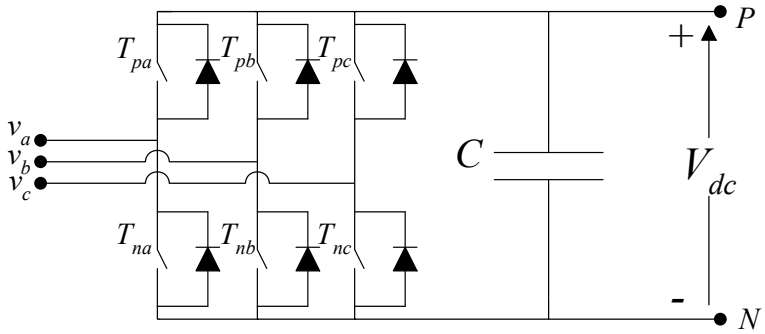

Figure 3.5: Voltage Source Converter.

Modulation of the transistors can be done in several ways. The two most frequently used techniques are space vector modulation (SVM) and carrier-based pulse width modulation (PWM). The first one, SVM, uses a strategy where the vectorial sum of the AC-voltages is controlled [15]. In PWM switching each phase voltage are controlled separately by its own control signal [14].

3.1.2 Application Areas

Historically, power electronic converters were predominantly used for domestic, industrial and information technology applications [16]. However, due to the development of power semiconductors and microelectronics devices, the decrease of the cost and advancement in processor technology, the application of VSC in power systems has gained a considerably more attention in the two past decades. Thus, applications of VSC now includes the area of power quality, HVDC system and flexible AC transmission system (FACTS) devices and electric drives system [17].

3.1.3 Pulse Width Modulation

In the classical carrier-based PWM the transistor are controlled based on a comparison between two signals. One signal is of a triangular waveform, v_{tri}, with a high frequency in range of several kHz. The other signal is the control signal, $v_{control}$, and it's dynamically generated by the control circuit according to the specified objectives [14]. $v_{control,a}$ is the control signal correspoding to phase a, and hence controls transistor T_{pa} and T_{na} in Figure 3.5. When $v_{control,a} > v_{tri}$ the T_{pa} transistor will conduct, and likewise the other transistor T_{na} will conduct when $v_{control,a} < v_{tri}$. In order to provide a sinusoidal output voltage the control signal, $v_{control,a}$, is chosen to be sinusoidal. Figure 3.6 shows the two signals and the resulting output voltage for one phase in a two-level converter. In a three-phase system three different control signals, one for each phase, are compared to the triangular pulse. The control signal hence controls the two transistors corresponding to its phase.

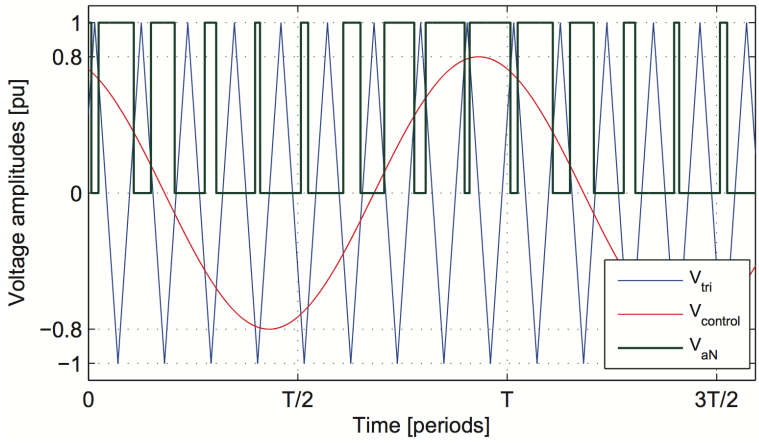

Figure 3.6: Pulse width modulation waveforms [12].

3.1.4 The Modular Multilevel Converter

Most VSCs are based on a two-level technology with the PWM control as the one presented above [18]. By two-level it is meant that the AC connection voltage can only be switched between two levels defined by the DC link capacitor. When the VSCs are used in HVDC applications this results in high and steep voltage steps at the AC connection terminal which generates severe electromagnetic interference. In order to reduce these effects multilevel converters has been introduced. They enables the feature of having a higher number of possible voltage levels that can be applied to the AC terminals. The result is a waveform closer to the sinus one, a reduction in switching frequency and a lower height and steepness of the voltage steps. However, as the voltage level and the power being transmitted is continuously increasing, these effects needs to be further improved. As a respond to this the modular multilevel converter (MMC) has been introduced.

The MMC is based on the concept that each converter arms can act as a controllable voltage source with a high number of possible discrete voltage steps [19]. Each of these variable voltage sources consist of a series connection of identical but individually controllable submodules. The principle is shown in Figure 3.7. The submodule is a two-terminal component which can be switched between full module voltage and zero module voltage in both current directions. A very smooth and nearly ideal sinus waveform is achieved, and hence less filter circuits are required [18].

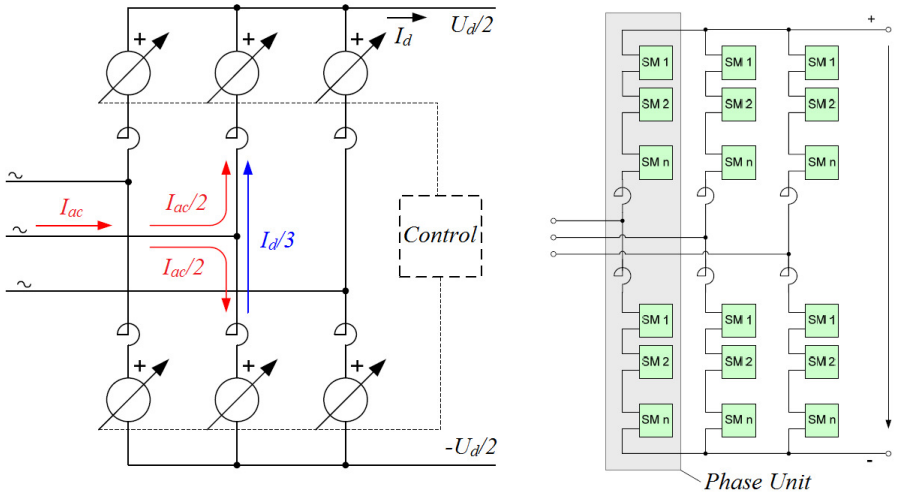

Figure 3.7: Overview of the MMC topology [18].

3.1.5 Detailed Model of VSC

Modeling the VSC can be done either in detail or by a a time-averaged approach. Detailed modeling of the VSC includes semiconducting devices and its properties such as blanking time, snubber circuits and on-state voltage drop [12]. A detailed modeling of the VSC requires highly advanced electromagnetic transient simulation tools such as PSCAD, ATM, PSIM or SimPowerSystems [13]. Figure 3.8 shows the per-phase equivalent of the converter including a resistance R and inductance L between converter and the connection point. A detailed modeling of the VSC is used for analyzing PWM techniques, different VSC topolgies, high frequency harmonic components and for accurate study of VSC losses.

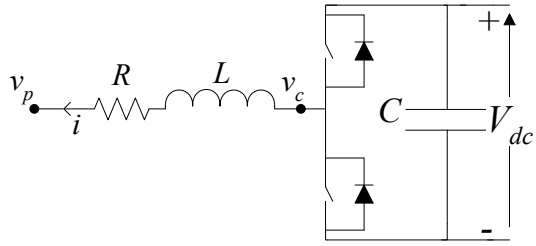

Figure 3.8: Per phase converter equivalent of the detailed model [12].

3.1.6 Average Model of VSC

For this system an average model is chosen. As the switching frequency approaches infinity, the converter output will be pure sinusoidal with no harmonics, and hence the converter can be modelled as a controlled voltage source [20]. The DC-circuit is connected to a controllable current source. Figure 3.9 shows how the two-level VSC can be modelled by using an average approach. The computational time for simulations are heavily reduced with the average model, and since neither harmonics, fast transients nor switching losses are going to be studied, the average model is more than sufficient enough for this thesis.

$v_{c,a}$, $v_{c,b}$ and $v_{c,c}$ refers to the three phase voltages generated by the VSC and i_a, i_b and i_c refers to the resulting phase currents flowing from the AC grid into the VSC. R and L represents the resistance and inductance of the series connected AC filter of the VSC while C is the DC-bus capacitance which act as a shunt filter [13]. I_c is the current injected into the DC grid by the VSC while V_{DC} and I_{DC} represents the DC-bus voltage and current that flows into the DC-cable.

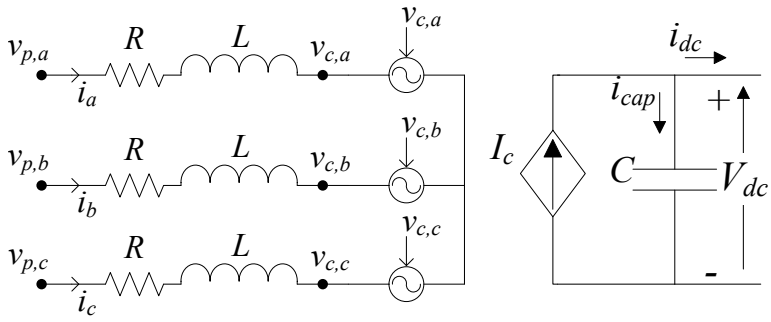

Figure 3.9: Voltage source converter average model.

The AC and DC circuits of the time averaged VSC model are related by the conservation of power. The voltage sources and current sources are hence controlled based on the following equation for the left side of the VSC in Figure 3.9.

$$v_{c,a}(t) \cdot i_a(t) + v_{c,b}(t) \cdot i_b(t) + v_{c,c}(t) \cdot i_c(t) = I_c(t) \cdot V_{DC}(t) \tag{3.7}$$

3.1.7 Control of VSC

Depending on the application of the VSC different control strategies and objectives are used. In this section a brief introduction to the control stratgies and structures of a VSC is given. A general model established in [12] will be presented and serve as a base for the control systems in the different applications of VSC.

The VSC has two degrees of freedom at each terminal, meaning that two variables can be controlled independently [12]. A commonly used technique to achieve independent control of the variables is namely the vector control. The vector control technique is based on the a synchronous rotating dq-reference frame. The direct-quadrature-zero (dq0) transformation, or Park transformation, is a mathematical transformation which rotates the stationary coordinate system (abc) [21]. The idea is to transform the sinusoidal waveforms into DC-quantities. The main reason for this is that the time-varying inductances will be constant in the dq-coordinate system [22]. Another advantage is that DC-quantities have smaller variations than sinusoidal and hence are easier to control and simulate. The mathematical approach is explained in Appendix A.1.

In order to simplify the control design a cascaded system is used. The full block diagram in Figure 3.10 shows the simplified representation of d-axis and q-axis current controllers. It consist of the control system, the converter and the electrical system. Neglecting the harmonics the electrical system will be described by means of the following general equations in the Laplace-domain [12]:

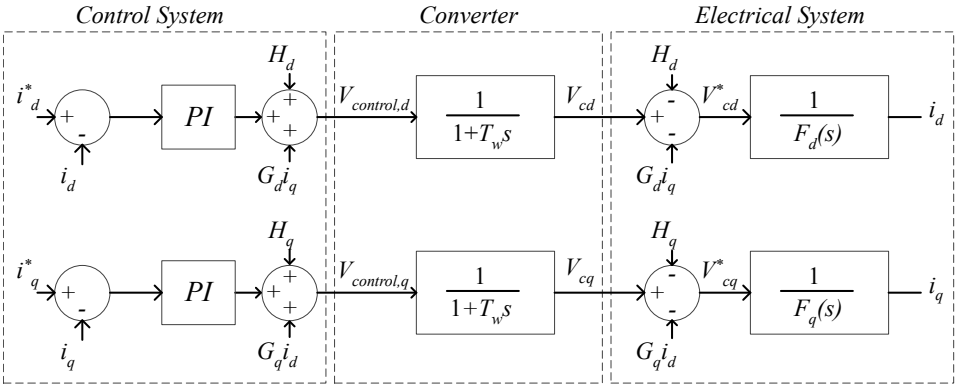

Figure 3.10: The general dq-current controller [12].

$$\begin{aligned} V_{cd} &= F_d(s) \cdot i_d + G_d \cdot i_q + H_d \\ V_{cq} &= F_q(s) \cdot i_q + G_q \cdot i_d + H_q \end{aligned} \tag{3.8}$$

where $V_{c,dq}$ is the voltage at the converter terminal and i_{dq} is the line current. $F_{dq}(s)$, G_{dq} and H_{dq} are arbitrary functions that is independent on i_d and i_q. $F_{dq}(s)$ represents a general impedance, G_{dq} represents the connection between the d- and q-axes, while as H_{dq} represents a general voltage located behind the impedance represented by $F_{dq}(s)$. Figure 3.11 shows the equations represented as an electrical equivalent circuit.

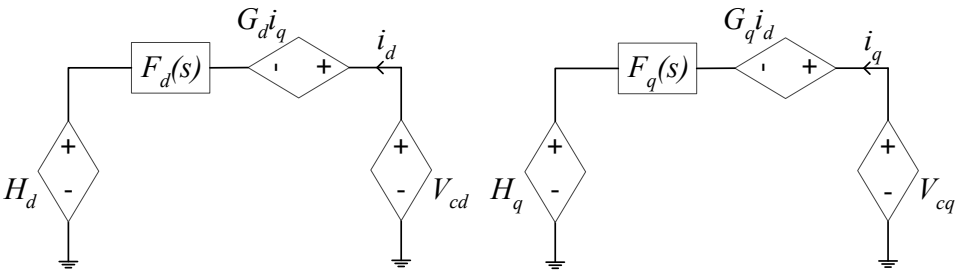

Figure 3.11: General equivalent system in the dq-reference frame [12].

The use of dq-reference frame in the control design and implementation enables to make a fully decoupled linear control of active and reactive currents [13]. The equations are therefore used to create a linearized model of the system. As seen in Figure 3.10 the main objectives with the control are to let i_d and i_q follow their corresponding references i_d^* and i_q^*. Due to the sinusoidal pulse width modulator the converter has a time delay of $T_w = \frac{1}{2f_s}$ where f_s is the switching frequency. The converter controls the voltages V_{cd} and V_{cq} and is expressed as follows in the

Laplace domain:

$$\begin{aligned} V_{cd} &= \frac{1}{1+T_w s} V_{control,d} \\ V_{cq} &= \frac{1}{1+T_w s} V_{control,q} \end{aligned} \tag{3.9}$$

where the control voltages, $V_{control,d}$ and $V_{control,q}$, are the desired voltages decided by the control system.

By looking at Figure 3.11 the control structure can be described. From equations 3.8 two variables are defined [12]:

$$\begin{aligned} V_{cd}^* &= V_{cd} - G_d \cdot i_q - H_d = F_d(s) \cdot i_d \\ V_{cq}^* &= V_{cq} - G_q \cdot i_d - H_q = F_q(s) \cdot i_q \end{aligned} \tag{3.10}$$

where V_{cd}^* and V_{cq}^* are linear with respect to the currents i_d and i_q. This makes the design of the PI-regulator easier. In order to obtain the desired converter voltage, $V_{control,dq}$, both $G_{dq} \cdot i_{dq}$ and H_{dq} are added to the regulator output. The voltage will appear as $V_{c,dq}$ at the converter terminals after the time-delay T_w. The physics in Equation 3.8 is represented by the summation to the right in Figure 3.10. If the time-delay, T_w, is so small that it can be neglected, the two summation blocks in Figure 3.10 will cancel each other out. The result is that only the transfer function F_{dq} remains between the regulator and the feedback.

3.2 Wind Aerodynamics

The aerodynamic processes related to wind turbines and the design of the rotor blades are highly complex and will not be studied in this thesis. Shortly explained, the blades are designed such that the wind that strikes the blades will create a torque in the direction of rotation. The speed of the air decreases resulting in a loss in energy. The loss in energy of the wind mass has been converted to rotational kinetic energy. For modelling the energy conversion a simple empirical model will be used.

The total wind power P_w that strikes a wind turbine are determined by the size of the wind turbine and the wind speed according to Equation 3.11 [23].

$$P_w = \frac{1}{2} \rho A V_w^3 \tag{3.11}$$

where $A = \pi R^2$ is the turbine cross section area, V_w is the mean wind speed over the turbine surface and ρ is the air density.

The power extracted by the wind turbine from the available power in the wind is decided by a performance coefficient, C_p [23]. A turbine cannot extract more than 59% of the total available power in the wind. This maximum theoretical limit

is known as the Betz limit. The mechanical power extracted from the wind is then given by Equation 3.12.

$$P_m = \frac{1}{2} C_p \rho A V_w^3 \tag{3.12}$$

The performance coefficient, C_p, is a function of the tip speed ratio, λ, and pitch angle, β. The tip speed ratio, given in Equation 3.13, is a function of the rotational speed of the turbine, ω_m, the wind speed, V_w, and the radius, R, of the turbine.

$$\lambda = \frac{\omega_m R}{V_w} \tag{3.13}$$

The power coefficient, C_p, can be expressed by [24]

$$C_p(\beta, \lambda) = 0.5176 \left(\frac{116}{\lambda_i} - 0.4\beta - 5 \right) exp^{-\frac{21}{\lambda_i}} + 0.006795\lambda_i \tag{3.14}$$

where λ_i is given by

$$\lambda_i = \frac{1}{\frac{1}{\lambda + 0.08\beta} - \frac{0.035}{\beta^3 + 1}} \tag{3.15}$$

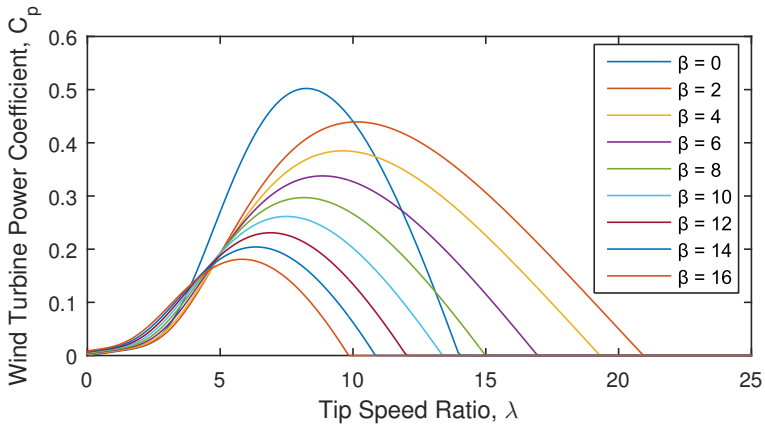

Figure 3.12: C_p as a function of λ for different pitch angles.

The variation of C_p as function of λ for different values of β is shown in Figure 3.12. The highest possible value of C_p is obtained when operating with β equal to zero degrees. Based on the above equations, a wind aerodynamic model can be made. The model will have wind speed, pitch angle and turbine speed as inputs and the power as an output, see Figure 3.13.

In Figure 3.14 the power extracted from the wind is shown as a function of the

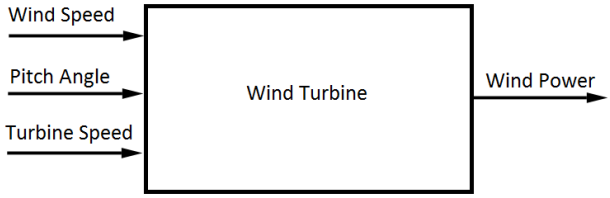

Figure 3.13: Wind aerodynamic block diagram.

turbine speed for different wind speeds. The pitch angle, β, is set to zero for all the curves. From this figure it is shown that the turbine should be able to operate at different rotational speeds in order to track the maximum operation point for different wind speeds.

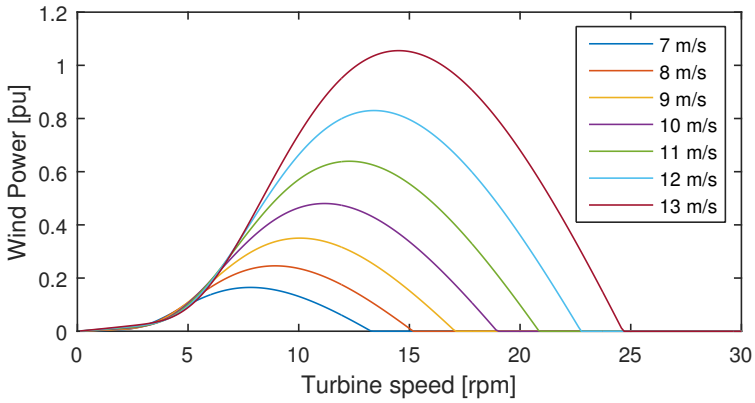

Figure 3.14: Power as a function of the turbine speed.

3.3 Maximum Power Point Tracking

In order to fully realize the benefits of variable speed wind power generations systems (WPGS), it is critical to develop advanced control methods to extract maximum power output of the wind turbines at variable wind speeds [25]. As already mentioned, the mechanical power output at a given wind speed is dependent of the turbine's tip speed ratio (TSR), and hence the turbine speed has to change as the wind speed changes in order to maintain the optimal TSR. Previous research has proposed several MPPT techniques. A comprehensive review and critical analysis of these techniques has been given in [26]. In this section the four most common techniques for maximum power extraction will be presented. These are the TSR

control, optimal torque (OT) control, power signal feedback (PSF) control and hill climb search (HCS) control. The three first techniques fall into the same category, namely the lookup table based category, and is the most used MPPT technique in WPGS today.

3.3.1 Tip Speed Ratio Control

The TSR control regulates the rotational speed of the generator in order to maintain the optimal TSR [25]. This method requires both the wind speed and the turbine speed to be measured. Knowing these to two variables and the optimal TSR, the system will be able to extract the maximum possible power. However, measuring the wind speed has been proven to be difficult [27]. An anemometer installed close to the wind turbine won't measure the accurate wind speed since the wind turbine will experience different forces due to wake rotation. In addition to the difficulties with the practical implementation of the wind speed measurement, it also adds severe costs to the system if all turbines should have this installed. Another drawback with this control method is that the optimal TSR is different from one system to another. Hence the control system has to be custom-designed for each turbine-generator characteristic. The control system is shown in Figure 3.15.

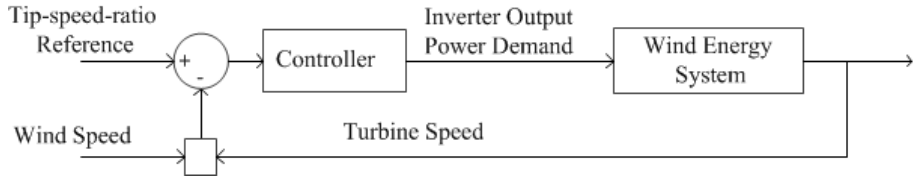

Figure 3.15: Block diagram of TSR control.

3.3.2 Optimal Torque Control

The OT control has the same goal as TSR control, namely maintaining an optimal TSR for the system. The different is that now the control system tries to adjust the torque according to a maximum power reference torque of a wind turbine at a given wind speed [28]. The control system is represented in Figure 3.16. The optimal reference torque can be determined as a function of the generator speed, ω_m, by first rewriting 3.13 accordingly:

$$V_w = \frac{\omega_m R}{\lambda} \tag{3.16}$$

Then by substituting Equation 3.16 into Equation 3.12 and replacing $\lambda = \lambda_{opt}$ and $C_p = C_{p,max}$ the following expresseion os obtained:

$$P_{w,opt} = \frac{1}{2}\rho\pi R^5 \frac{C_{p,max}}{\lambda_{opt}^3}\omega_m^3 = K_{p,opt}\omega_m^3 \tag{3.17}$$

Then considering the relation between the power and the torque, $P_g = T_m\omega_m$, the optimal torque as a function of the generator speed is given as followed:

$$T_{m,opt} = K_{p,opt}\omega_m^2 \tag{3.18}$$

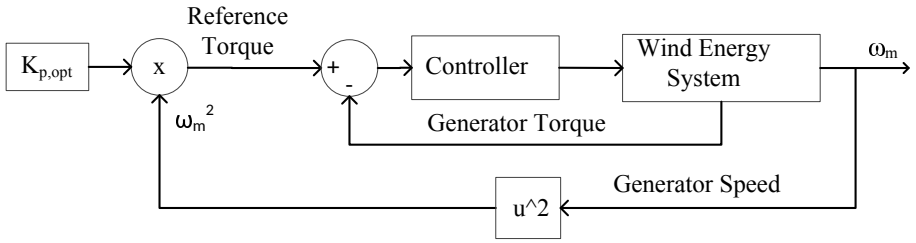

Figure 3.16: Block diagram of OT control.

The optimal torque curve, which is given as a reference torque for the wind turbine controller, is shown in Figure 3.17. This method is simple, fast and efficient. However, since it does not measure the wind speed directly wind changes are not reflected instantaneously and hence the TSR control method is more efficient [28]. It is also an expensive control method to implement since the maximum power curve, and hence the optimal torque curve, needs to be obtained through simulations or tests for individual wind turbines.

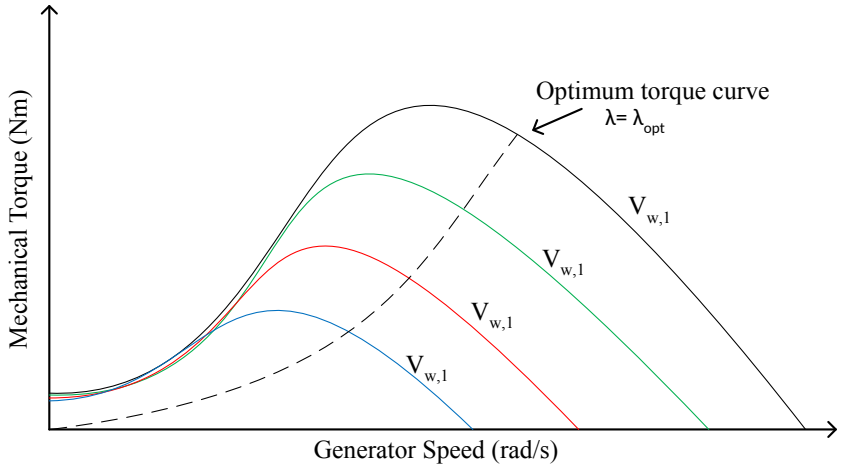

Figure 3.17: Torque-speed characteristic curve for a series of wind speeds.

3.3.3 Power Signal Feedback Control

The PSF control method uses the optimal power curve given in Equation 3.17 as a reference, and hence it operates in a similar way as the OT control. Figure 3.18 shows the block diagram for the PSF control signal generation. There is no difference in the performance and complexity of implementation between the PSF and OT control methods [26]. They both have the advantage with no necessity of an anemometer for wind speed measurement and the disadvantage of the same slow regulation.

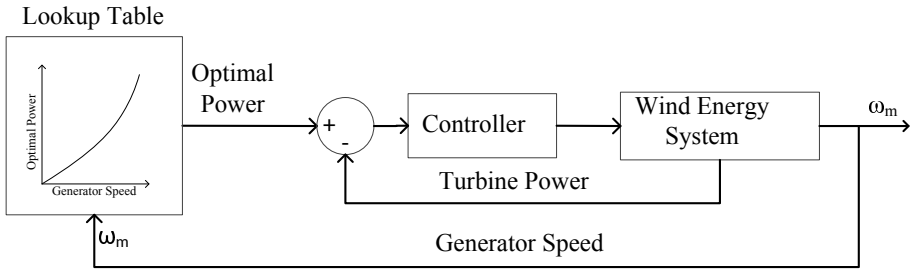

Figure 3.18: Block diagram of PSF control.

3.3.4 Hill Climb Search Control

In order to overcome the above mentioned drawbacks with the lookup table based control methods the HCS control has been proposed. The control method is also known as perturb and observe control method as it is perturbing the control variable and observing the result [26]. In this case the control variable will be the generator speed while the result will be the power generated. If an increase in generator speed results in an increase in generated power, the same perturbation is repeated, otherwise the sign of the perturbation is reversed and the speed is then lowered. The principle can be shown in Figure 3.19 and expressed mathematically as in Figure 3.19.

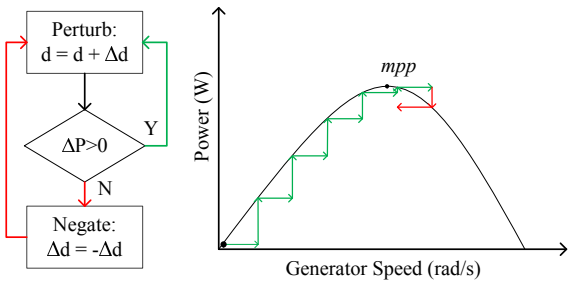

Figure 3.19: Principle of the HCS control technique [26].

HCS control is a simple an flexible MPPT method as it doesn't require any prior knowledge of the system or any additional sensors. It is therefore a good alternative to system that has a unique power maximum, as for example renewable energy conversion systems. However, it fails to reach maximum power points for large inertia wind turbines under rapid wind variations. There are especially two serious problems with the HCS control that occurs under rapidly changing wind conditions [26]. The first problem is associated with the size of the perturbation step-size and is shown in Figure 3.20. A larger step-size will increase the speed of convergence but it will also give more oscillations around the maximum power point (MPP) and hence have a negative effect on the efficiency. With a smaller step-size one will improve the efficiency but reduce the convergence speed and hence it may be incapable of tracking the MPP under the varying wind conditions.

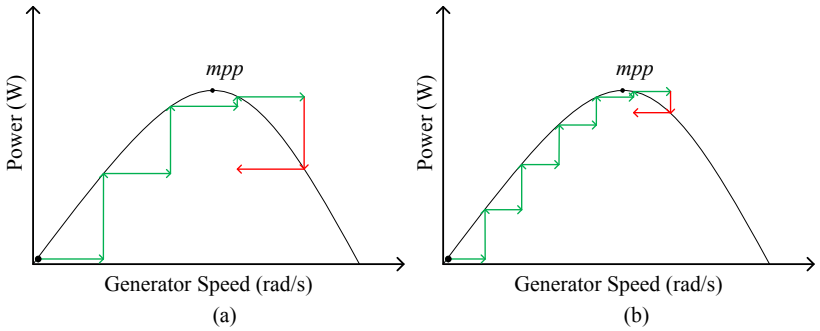

Figure 3.20: HCS control with different step size [26].

The second problem is that the controller cant distinct whether the power increase or decrease is due to the previous perturbation or due to a change in wind speed. Figure 3.21 shows how this may lead to a wrong decision in determining the next perturbation. Instead of moving uphill towards the MPP it ends up moving downhill which results in a lower efficiency.

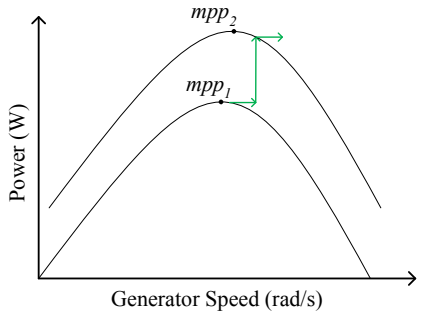

Figure 3.21: HCS control during an increase in wind speed.

3.4 Permanent Magnet Synchronous Generator

In order to understand how the PM synchronous machine is working, a mathematical model based on the stator voltage equation is presented. The dynamic equations for the generator, given in the abc reference frame, are as follows:

$$\vec{V}^s_{abc} = R_s \vec{I}^s_{abc} + \frac{d}{dt}\vec{\lambda}^s_{abc} \tag{3.19}$$

where V^s_{abc} is the stator phase voltage, R_s is the stator winding resistance per phase, I^s_{abc} is the stator phase current and λ^s_{abc} is the flux linkage [22].

In order to have a simpler model a transformation from abc to dq rotating reference frame is done. An explanation of the abc to dq transformation is included in Appendix A.1. An illustration of this model is shown in Figure 3.22, were d-axis is always aligned with the rotor magnetix axis, with the q-axis 90° ahead in the direction of rotation, assumed to be counter-clockwise.

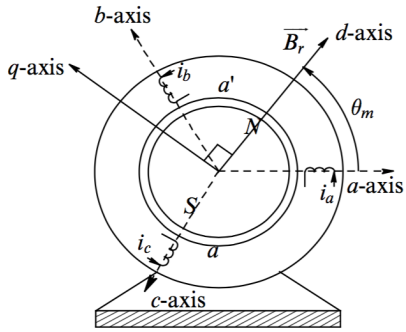

Figure 3.22: Permanent magnet synchronous machine with two poles [22].

The stator voltage equations in the dq synchronous reference frame are then represented as

$$\begin{aligned} v^s_d &= R_s i^s_d + \frac{d}{dt}\lambda^s_d - \omega_e \lambda^s_q \\ v^s_q &= R_s i^s_q + \frac{d}{dt}\lambda^s_q + \omega_e \lambda^s_d \end{aligned} \tag{3.20}$$

where v^s_d and v^s_q are the dq axis stator voltages, i^s_d and i^s_q are the dq axis stator current, λ^s_d and λ^s_q are the dq axis stator flux linkages, R_s the stator resistance and ω is the electrical speed in rad/s. The electrical speed, ω, is related to the actual rotor speed, ω_{mech}, as presented in Equation 3.21

$$\omega = \frac{p}{2}\omega_{mech} \tag{3.21}$$

where p is the number of poles.

In a synchronous machine with surface-mounted permanent magnets the rotor can be considered magnetically round, non-salient, which means that it has the same reluctance along any axis through the center of the machine. The stator d and q winding flux linkages can then be expressed as follows

$$\begin{aligned} \lambda_d^s &= L_s i_d^s + \lambda_{fd} \\ \lambda_q^s &= L_s i_q^s \end{aligned} \tag{3.22}$$

where $L_s = L_{ls} + L_m$ is the sum of the leakage inductance and the magnetizing inductance, and λ_{fd} is the flux linkage of the stator winding due to flux produced by the rotor magnets. When inserting Equation 3.22 into Equation 3.20 and rearranging it can be written in the Laplace domain in order to match Equation 3.8 [12]:

$$\begin{aligned} v_{cd} &= \underbrace{(R_s + sL_s)}_{F_d(s)} i_d + \underbrace{-\omega L_s}_{G_d} i_q + \underbrace{0}_{H_d} \\ v_{cq} &= \underbrace{(R_s + sL_s)}_{F_q(s)} i_q + \underbrace{\omega L_s}_{G_q} i_d + \underbrace{\omega \lambda_{fd}}_{H_q} \end{aligned} \tag{3.23}$$

The corresponding equivalent circuit is shown in Figure 3.23, and is analogous to the general equivalent circuit presented in Figure 3.11.

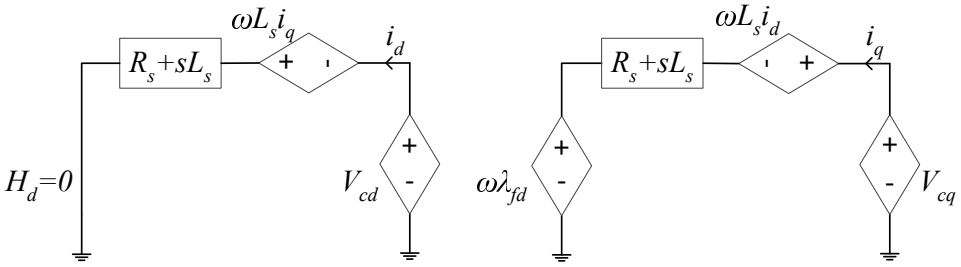

Figure 3.23: PMSG circuit equivalent in dq-frame [12].

The electromagnetic torque for a PMSG is given by Equation 3.24 [29].

$$T_{em} = \frac{3}{2}\frac{p}{2}(\lambda_d^s i_q^s - \lambda_q^s i_q^s) \tag{3.24}$$

Substituting for flux linkages in the equation above, the electromagnetic torque for a nonsalient-pole machine becomes

$$T_{em} = \frac{3}{2}\frac{p}{2}\lambda_{fd} i_q^s \tag{3.25}$$

The difference of the electromagnetic torque and the load torque which is acting

on the combined inertia of the machine and the load, J_{eq}, gives the acceleration of the machine [22].

$$\frac{d}{dt}\omega_{mech} = \frac{T_{em} - T_L}{J_{eq}} \tag{3.26}$$

where ω_{mech} is in rad/s and related to ω as shown in Equation 3.21. Equation 3.26 can also be written in terms of the per-unit system. The inertia of the machine, J_{eq}, is then represented as $2H$, where H is the inertia time constant.

3.5 Control of the PMSG

In this section a brief introduction to the state of the art interaction between the PMSG and the converter will be given. In this thesis only the interaction with the generator side converter (GSC) is studied. There is a lot of research done towards this topic and several methods are proposed. Figure 3.24 shows the block diagram of a wind turbine and the GSC, as well as one of these control methods. Similar approaches to PMSG control in wind turbine has been given in the references [12], [30] and [31]. The method used in this case are based on the assumption that the wind speed are measured. As this is very difficult, as already mentioned, it can also be estimated with sensorless control as used in the references [32] and [33].

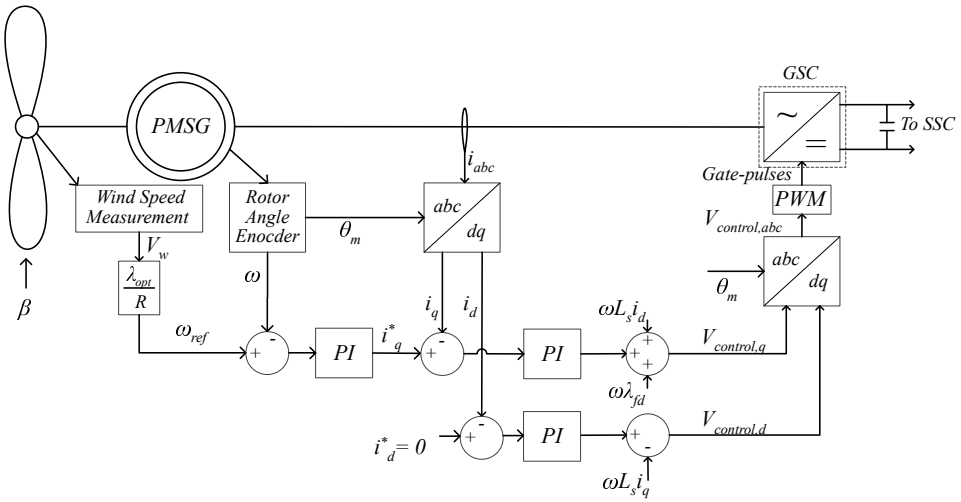

Figure 3.24: Generator side converter with control [12].

In Figure 3.24 the rotor speed and position are measured along with the generator currents. The rotor angle is used in the Park-Transformation as the transformation angle is required to be aligned with the rotor flux, λ_{fr} [12]. The current control system can be recognized from the method presented in Section 3.1.7 and

in Figure 3.10. The arbitrary functions F_{dq}, G_{dq} and H_{dq} are found from Equation 3.23. The reference current for i_d can either be set to zero in order to minimize the total current in the stator, and hence also minimize the resistive losses, or it can be used to minimize the sum of all losses in the generator as done in [30]. Based on the MPPT methods presented in Section 3.3 the GSC can achieve maximum power extraction from the wind. In order to achieve optimal TSR the GSC needs to control the generator speed. This is done by controlling the electrical torque as the quadrature current, i_q, is dependent on the torque according to Equation 3.25. The deviation between the measured speed and the calculated optimal speed is applied to a PI-controller giving the quadrature reference current, i_q^*, as an output.

3.6 System Side Control

The objectives of the system side control (SSC) are to control the DC-link voltage, V_{DC}, and the reactive power, Q, to the grid. A complete schematic of the converter and the control system are shown in Figure 3.25.

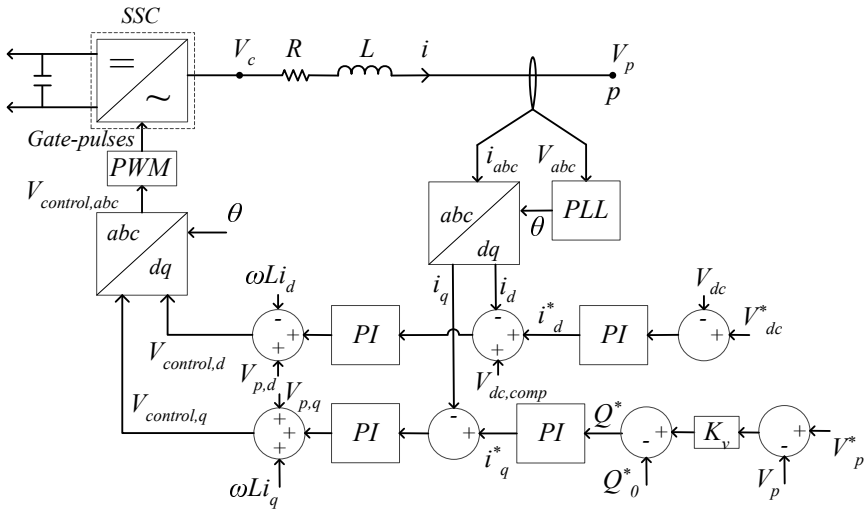

Figure 3.25: System Side Converter (SSC) with control [12].

The complete control structure are similar to the GSC and hence the same notation as presented in Section 3.1.7 will be used. This results in the following model of the converter and grid [12] [34]:

$$
\begin{aligned}
v_{cd} &= \underbrace{(R_s + sL_s)}_{F_d(s)} i_d + \underbrace{-\omega L_s}_{G_d} i_q + \underbrace{v_{pd}}_{H_d} \\
v_{cq} &= \underbrace{(R_s + sL_s)}_{F_q(s)} i_q + \underbrace{\omega L_s}_{G_q} i_d + \underbrace{v_{pq}}_{H_q}
\end{aligned}
\tag{3.27}
$$

where $v_{c,dq}$ is the voltage at the converter terminals while $v_{p,dq}$ is the voltage at the connection point, i_{dq} is the line current flowing out of the converter and ω is system frequency in rad/s. The inductance L and the resistance R represents the filter between the converter and the point of connection. The equivalent circuit of Equation 3.27 is shown in Figure 3.26 which is based on the general circuit in Figure 3.11 presented in Section 3.1.7.

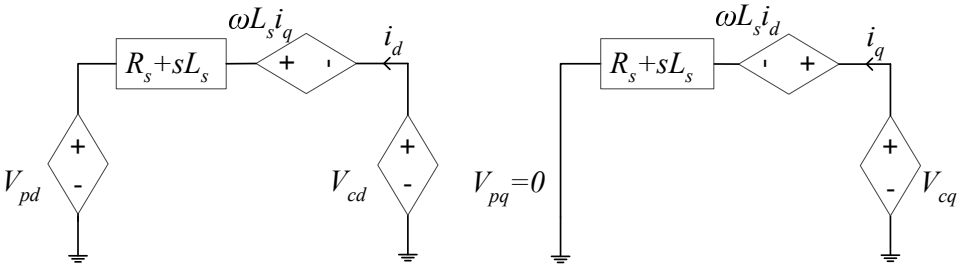

Figure 3.26: SSC circuit equivalent in dq-frame [12].

By choosing the phase angle in phase A of V_p as the transformation angle the voltage V_{pq} will be zero which is a useful property in the control system [12]. The angle is calculated by a Phase-Lock-Loop (PLL) based on the measured voltage at the point of connection.

3.7 Cable modelling

For short lines, or cables, and low voltage levels the capacitance of the lines can be ignored without much error [35]. For longer cables and higher voltages it is no longer sufficient to only include the series impedance. As the length of the line increases, the line charging current becomes appreciable and the shunt capacitance must be considered. For the transmission cable, the resistance, inductance and capacitance are uniformly distributed along the cable. An approximate model of the distributed parameters is obtained by using several identical π-equivalents. The π-equivalent is shown in 3.27.

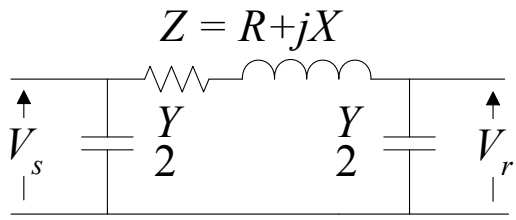

Figure 3.27: π-equivalent of a transmission line.

Z is the total series impedance of the cable, and Y is the total shunt admittance of the line given by

$$Y = j\omega Cl \tag{3.28}$$

where C is the line-to-neutral capacitance per km, and l is the length of the line in km.

The capacitance and inductance of a cable, given in $\mu F/km$ and mH/km, are usually found in data sheets provided by the manufacturer of the cable. Along with these values, one will also find the charging current, given in A/km at a specified frequency, and the physical measurements of the cables cross-section. The resistance however, will vary as it is dependent on the operating temperature of the cable [36]. It is also dependent on the material of the conductor, the length and the cross-sectional of the conductor according to Equation 3.29.

$$R_0 = \frac{\rho l}{A} \tag{3.29}$$

R_0 is the resistance in ohms at 20 °C, ρ is the resistivity of the material in ohm meter and l is the length in meter. When taken into account that the cable is operating at another temperature, θ, the resistance, R, of the cable is given by

$$R = R_0\Big(1 + \alpha\big(\theta - 20°C\big)\Big) \tag{3.30}$$

where α is the temperature coefficient for the conductor material. In Table 3.1 both the resistivity, ρ, and the temperature coefficient, α, for Copper and Aluminium are listed.

Table 3.1: Material properties.

	ρ	α
Copper	$1.68 \cdot 10^{-8}$	0.003862
Aluminium	$2.82 \cdot 10^{-8}$	0.0039

3.8 Variable Transmission Voltage

Another option for loss minimization in long offshore wind farm AC export cables is to vary the transmission voltage as proposed in [37]. The option is motivated by the fact that the cable losses due to the charging currents decreases with decreasing voltage. When the wind farm production is low the losses due to charging current may dominate over those of the transmitted power. The voltage of the export-cables can be varied by use of transformer on-line tap changers. In [37] it is shown how this can both reduce cable losses and extend the technical range limits of the AC cable for an 320 MW wind farm connected to shore via a 200 km cable at 220 kV nominal voltage. By simply using a ±15% tap changer voltage regulation on the two transformers an annual loss reduction of 9% is achievable [37].

There are two strategies that has been proposed. The first one is to operate at a fixed, optimized voltage. And the second one is to operate at a varying voltage that is continuously optimized for the instantaneous power production in the wind farm. The cable efficiency for the two strategies found in [37] can be shown in Figure 3.28.

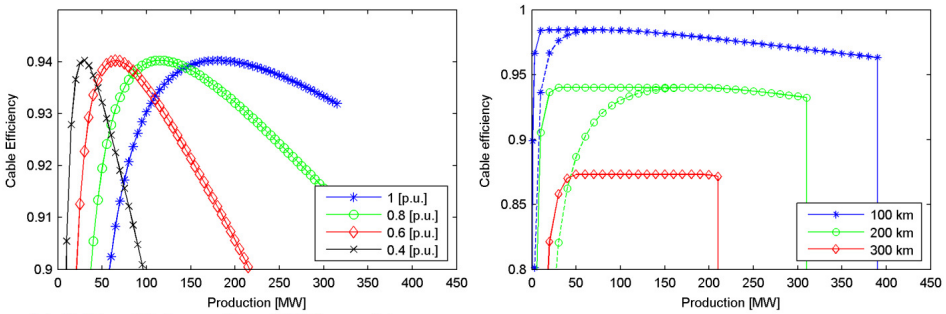

(a) Cable efficiency for a 200 km cable with different operating voltage.

(b) Cable efficiency for different cable lengths with operation at optimal (variable) voltage.

Figure 3.28: Cable efficiency as a function wind farm instantaneous active power production for both strategies. In (b) the solid lines are operations at optimal (variable) voltage and dashed lines for operation at 1.0 pu fixed voltage [37].

3.9 Compensation

As already mentioned in Section 2.2, HVAC cables leads to substantial charging currents due to the high capacitance. The capacitance of cable is 10-20 times higher than the capacitance on an equivalent overhead line [38]. The capacitance and charging currents will increase linearly with the length of the cable [39]. Such high charging currents results in a high generation of reactive power by the cable which needs to be consumed in order to keep the voltage within acceptable values

and to ensure the cables efficiency. Consumption of this reactive power is achieved by using shunt reactors. Shunt reactors consist of an inductive reactance whose purpose is to draw reactive power from the system [38]. The charging current per phase, I_c, is defined by the following equation:

$$I_c = UC\omega l \tag{3.31}$$

where U is the phase voltage, C is the capacitance per length of the cable, ω is the angular frequency and l is the length of the cable. The total reactive power generated by the shunt capacitance in the cable is given by:

$$Q_C = 3I_cU = 3\omega ClU^2 \tag{3.32}$$

The shunt reactor will consume reactive power generated by the cable according to the following equation:

$$Q_L = 3I_LU = 3\frac{U^2}{\omega L} \tag{3.33}$$

where L is the inductance of the shunt reactor. By decreasing the value of the inductance the reactive power consumed will increase. The voltage drop is not equal along the cable, hence the reactive power consumed will change as a function of the position. By choosing the right compensation level and the right placement of the shunt reactors, the Ferranti effect can be decreased [39]. Figure A.2 in Appendix A.2 illustrates the loading of an open ended line due to the charging current for different arrangements of compensation level and placement.

For an offshore cable the only relevant solutions are the two first alternatives in Figure A.2, with the second alternative as the best suited one. The worst alternative will bee when the compensation is only placed at one end. By equally distributing the compensation at both ends, the charging current at the most loaded points will be reduced to half of the value compared to the first alternative.

One important feature to notice, and that has to be considered when a cable and a shunt reactor are exposed to a variable frequency system, is that they react different to the changes in the frequency. The reactive power generated in the cable will become smaller when the frequency drops. In the shunt reactors however, the amount of reactive power it will draw increases. As a result of this the system will require an even more active compensation, meaning that the reactive power compensated for should be controlled based on the amount of reactive power generated in the cable.

FACTS devices

A system composed of static equipment based on power electronics are usually referred to as flexible AC transmission systems (FACTS) while the electronic devices

themselves are referred to as FACTS devices [40]. The devices consists of a controlled semiconductor, namely a thyristor. Static VAR compensators (SVCs) are part of the FACTS device family and has the role of adjusting the amount of reactive power compensation the system needs. Using thyristor controlled shunt elements a flexible and continuous reactive power compensation can be achieved. By using the thyristor controlled reactor (TCR) in parallel with a bank of shunt capacitors a flexible and continuous reactive power compensation operating in both capacitive and inductive region can be achieved. The use of such devices will therefore help overcome the above mentioned challenge with the varying need of compensation. At the cable terminals a standard TCR would then be able to reduce the amount of reactive power consumed. If the SVC also would require to operate in the capacitive region the TSR should be in parallel with a capacitor bank. The SVC would then be able to regulate the voltage at its terminals by controlling the reactive power injected into the system or absorbed from the system. At lower voltages the reactor would be switched fully off and the SVC would be capacitive and hence generate reactive power. When the voltage level is high the reactor is switched on resulting in a net inductive SVC that absorbs reactive power.

Chapter 4

System Overview

This chapter will present the proposed system and the model along with its components. The model in this thesis is made in MATLAB R2015a and the integrated softwares Simulink, Simscape and SimPowerSystems. Section 4.1 will describe the proposed system which has been studied in this thesis. Then the model and the different components are presented in section 4.2.

4.1 The Proposed System

The proposed turbine concept is a result of the trend of making the wind turbines bigger and cheaper in addition to also make the transmission system cheaper and more effective. As mentioned in Section 2.2.2, the HVDC transmission system has been considered as the best alternative due to the increasing distance to shore and power being transmitted. However, as the trend now is to use large direct driven generators which operates at a low rpm they can produce a low frequency alternating current directly. By merging this idea with the LFAC transmission system a new concept has been proposed. Instead of installing a frequency converter in the turbine, the generator can be used to output this frequency directly. Excluding the offshore converters leads to high potential cost savings. However, it will result in loss of controllability and hence loss of potential power. The reason is that with no converters in between the different turbines, they all have to operate at the same speed. The interesting option with this topology is that by controlling the frequency in the transmission cable from the onshore converter station one will be able to control the entire wind farm. A sketch of the proposed system is shown in Figure 4.1. The wind turbines consists of large direct driven PMSGs without any converters.

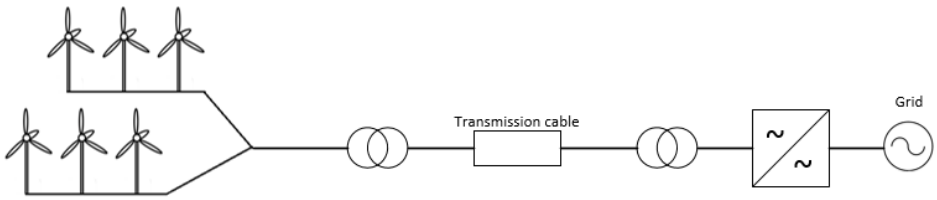

Figure 4.1: The proposed system.

4.2 The Model

The modeled system is shown in Figure 4.2. It consist of one NOWITECH[1] reference turbine with the installed power of 10 MW and the rated line to line voltage of 4 kV rms in parallel with an aggregated wind park equivalent of 190 MW. The wind turbine transformer steps up the voltage from 4 kV to 33 kV, which is the offshore collector grid voltage level. Then the power is being transmitted through cables of various lengths to the offshore substation. The offshore substation transformer steps up the voltage from 33 kV to the transmission voltage level of 220 kV. Another transformer is placed onshore which steps the voltage level further up to 380 kV before the connection to the onshore converter station. The final model made in SimPowerSystems is shown in Figure B.3 in Appendix B.3. The black buses in the model are used for voltage and current measurement in order to calculate the power flow in the system.

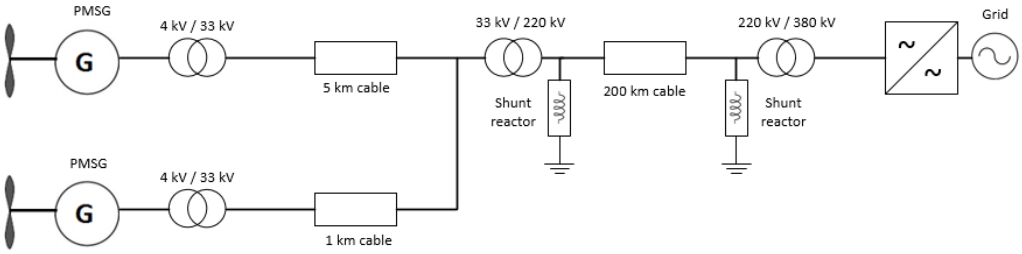

Figure 4.2: The modeled system layout.

4.2.1 The Wind Turbine Generator

In the proposed wind power system, the turbines are supposed to use PMSGs. In the model however, these are modelled as a synchronous machine with constant internal voltage and not as a PMSG as this simplifies the MATLAB modelling.

[1] See Appendix B.1 for information.

The synchronous machine blocks are compatible with the embedded load flow tool, which makes initializing the system easier, more about this in Section 4.3. This simplification is also made based on previous work done by Henrik Kirkeby in [41], where he also uses the NOWITECH 10 MW reference turbine. It was therefore found convenient to use the same data for the generator as him, which are actually based on standard values found in MATLAB Simulink. For further research, it is therefore recommended that more specific values for the reference turbine is used in order to achieve more accurate results. The same values are also used for the aggregated wind turbine generator except the power rating which is 190 MW. The parameters for the generators are shown in Table 4.1, given in per-unit (pu).

$R_s = 2.85 \cdot 10^{-3}$	$R_f = 5 \cdot 10^{-3}$	$R_{kq1} = 0.0287$
$L_l = 0.1$	$L_{lfd} = 0.1$	$L_{lkq1} = 0.2553$
$L_{md} = 0.5$	$R_{kd} = 0.0652$	$R_{kq2} = 7.765 \cdot 10^{-3}$
$L_{mq} = 0.4$	$L_{lkd} = 0.5134$	$R_{lkq2} = 0.9167$

Table 4.1: Generator parameters.

The rated rotational speed for the NOWITECH reference turbine is 13.54 rpm. For this project it is desired that the generator should output a frequency as close to 50/3 Hz as possible at rated speed. The relation between the generator speed, electric frequency and number of poles is given by Equation 4.1 [42].

$$n = \frac{120f}{p} \tag{4.1}$$

where n is the mechanical speed of the rotor in rpm, f is the electrical frequency in Hz, and p is the number of poles. By using this, it is found most convenient to change the rated speed to 13.51 rpm and use 148 poles. The time constant H is also found from the work done by Henrik Kirkeby in Appendix B in [41]. The time constant has been recalculated for the rated speed of this turbine.

$$\begin{gathered} H = 2.65\ s \\ p = 148 \\ f = 50/3\ Hz \end{gathered}$$

Table 4.2: The time constant, number of poles and rated frequency of the generator.

4.2.2 Offshore AC Collector Grid

The wind turbines transformers have a Δ-Y connection with an voltage ratio of 4kV/33kV. The transformer is rated for 10 MW with a power factor of 0.9, giving

$S_n = 11.11MVA$. For the aggregated wind park equivalent the transformer is rated for 190 MW, resulting in $S_n = 211.11$MVA. The winding resistance and leakage reactance are respectively assumed to be 0.002 and 0.08 pu. Magnetization resistance and inductance are both 500 pu. In order to connect the generator and transformer in series in the model, a large shunt resistance is coupled in parallel.

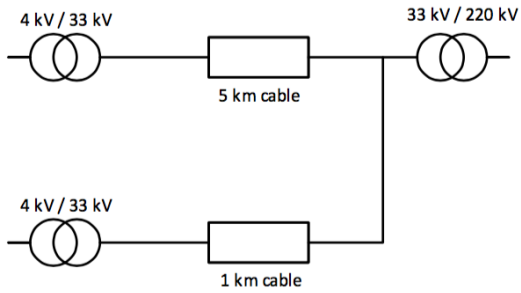

Figure 4.3: The offshore AC grid.

Rated voltage for the offshore collector grid is 33 kV. In this case there is only one collector point, which is at the substation as shown in Figure 4.3. Another option would be to have several wind turbines connected to one string before it was connected to the collector point. The cables are therefore rated for 10 MW each. This gives a rated current of 194 A. From ABBs XLPE Submarine Cable Systems data sheet [43], it is found from Table 33 that the cables need a cross section of 95 mm^2. A copper cable is chosen, and the parameters is found in Table 44 in the data sheet. The resistance has been calculated from the Equations 3.29 and 3.30 in Section 3.7 assuming maximum operating temperature of 90°C. The parameters for the cable are listed in Table 4.3.

$$R = 0.2246\ m\Omega/km$$
$$C = 0.18\ \mu F/km$$
$$L = 0.43\ mH/km$$

Table 4.3: The offshore collector grid cable parameters.

The cables are modeled using the π-equivalent, explained in Section 3.7. Since the aggregated wind turbine represents 19 wind turbines in parallel, the resistance, R, and inductance, L, of the cable is divided by 19 and the capacitance, C is multiplied by 19. The two wind turbines have different distances to the substation, 1 and 5 km. The main transformer, the one before the transmission cable to shore, has a rating 222.222 MVA and a voltage ratio of 33kV/220kV. The transformer has an Y-Y connection. The resistance is assumed to be 0.001 pu for both windings,

and the leakage inductance is 0.01 pu. Magnetization resistance and inductance are assumed to be 500 pu for this transformer as well.

4.2.3 The Transmission Cable

The transmission cable to shore is also modeled as a π-equivalent. The number of π-sections are chosen to be four due to its length of 200 km. The reason behind this is that the parameters are actually uniformly distributed along the cable. For short cables this will not be that important, but for longer cables this have to be considered, as mentioned in Section 3.7. By using four π-sections one will have a more realistic equivalent.

The data used for the copper cable are found in ABBs XLPE Submarine Cable Systems data sheet [43]. The cable was chosen to have a rating of 222.22 MVA at a voltage of 220 kV, which gives a rated current of 584 A. According to the data sheet, minimum cross section available at this level are $500mm^2$. The parameters of the cable is given in Table 49 in [43], and by making the same assumptions as for the offshore grid cables the values are found to be:

$$R = 0.1244\ m\Omega/km$$
$$C = 0.14\ \mu F/km$$
$$L = 0.43\ mH/km$$

Table 4.4: The transmission cable parameters.

A shunt reactor is needed in order to compensate for the reactive power generated in the cable. From Equation 3.32 it is found that the total reactive power generated in the cable is 141.92 MVAR. Based on the theory in Section 3.9 it is chosen to use two shunt reactors, one in both ends of the cable. The shunt reactors will then need to compensate for half of the generated reactive power each. From Equation 3.33 the inductance L of the shunt reactor is found to be 6.52 H. From the load flow analysis done in MATLAB SimPowerSystems the system is found to draw reactive power from the grid. As one wish to have a system that draws minimal of reactive power from the grid, the inductance L is increased to 9.576 H which reduces the compensation. An overview of the cable and the placement of the shunt reactors are shown in Figure 4.4.

4.2.4 Onshore System

When the cable reaches the onshore substation another transformer steps up the voltage for further transmission onshore. The transformer has an Y-Δ connection and is rated for 222.22 MVA, with voltage ratio of 220kV/380kV. The resistance and leakage inductance are assumed to be 0.001 and 0.01 respectively. Magnetization

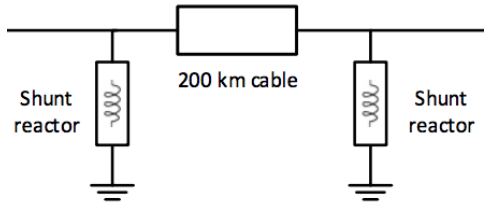

Figure 4.4: The transmission cable with shunt reactors.

resistance and inductance are again assumed to be 500 pu. Before the system can be connected to the grid, a frequency converter is needed. The converter is based on the theory presented in Section 3.1. As the scope of this thesis isn't to analyze different PWM techniques or different VSC topologies, such as various multilevel VSCs, the average model is used. The focus in this thesis have been to investigate the offshore side of the converter and the control of the wind turbines. Therefore, it is only the offshore side converter that has been modelled. This is modelled as three controllable voltage sources, one for each phase. The control concept of these sources will be presented in Chapter 5. In the rest of the thesis when referring to the grid, it is actually referring to the converter terminal.

4.3 Initializing the system

Before the simulations can be done the system have to be initialized. The SimPowerSystems library provides a special block for doing this, namely the Powergui-block, which should be further explained. The Powergui-block provides useful graphical user interface (GUI) tools to analyse the power system models [44]. The Powergui block is placed in the top level of the model in order to use the interface. The most important feature for this project is the "Load Flow" tool which has been used in this thesis. It allows one to perform load flows and initialize the three-phase network and the machines so that the simulations starts in steady state.

Chapter 5

Control Concept

This chapter will present the different control strategies implemented in the model and the blocks that were used to simulate this.

5.1 Wind Power Generation

The generators used in the model has a power input which needs to be controlled as the wind speed, and hence the power generated, in the system will vary. The amount of power extracted from the wind by the wind turbine are given by a performance coefficient as mentioned in Section 3.2. Based on three variables, the power input of the system can be calculated. In this thesis the pitch angle, β, of the blades are set to be zero and hence the wind speed used in the simulations will never exceed the rated wind speed of 13 m/s. In other words, it is assumed that in cases with higher wind speeds the blades would pitch out or stall and hence the power output would be the same as for doing this simplification. Based on the generator speed and the wind speed the amount of power can then be calculated by use of the formulas given in Section 3.2. This results in the block shown in Figure 5.1.

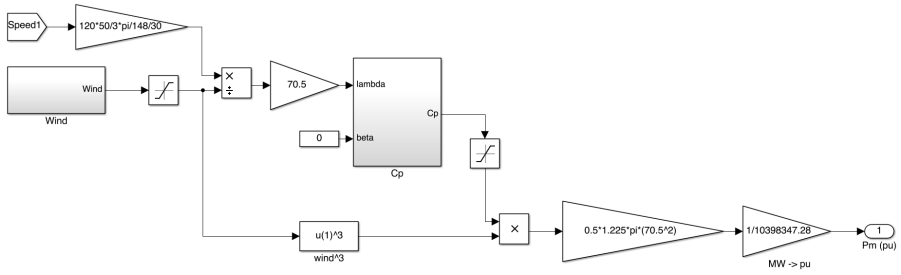

Figure 5.1: Wind power input block.

5.2 Frequency Control

The onshore converter should control the frequency of the offshore grid, the amplitude and hence reactive power exchange. In this thesis the focus has been on the frequency control and hence the magnitude has been considered constant. By controlling the frequency, one will also control the speed of the generators as seen from Equation 4.1. From the four MPPT control strategies presented in Section 3.3, PSF control and HCS control has been considered as the best options. The control strategy used in this thesis is mainly based on the PSF control. The lookup table used in the model is an inverse version of the one used in normal PSF control. Instead of controlling the power based on speed measurements, the frequency, and hence the speed, is controlled based on power measurement at the converter terminals. The block diagram used in the model is shown in Figure 5.2.

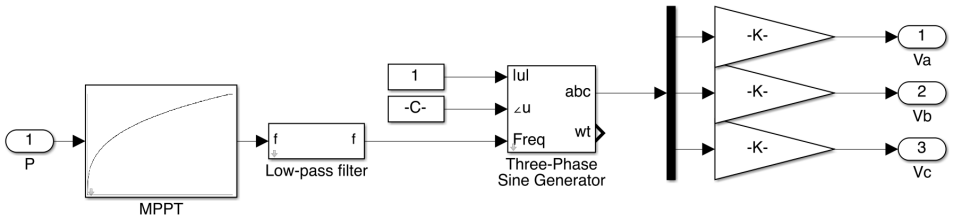

Figure 5.2: The frequency control block.

The lookup table is made based on calculations and simulations for the optimal speed versus power characteristic for one turbine. As this way of controlling a wind turbine is nothing like the known methods, one also has to take into consideration that there will be losses in the system. Even though the generators operates at maximum efficiency the active power delivered to the grid will be lower. A lower power level would imply that the optimal frequency is lower than the rated frequency and hence the control system would reduce the frequency. Therefore one has to take this loss into consideration in the frequency versus power curve in order to achieve an optimal operation when controlling it from shore. Through simulations the power loss in the system is found and thereby the maximum capable power exchange with the grid. This maximum will serve as base value for the onshore power measurement ensuring an optimal frequency.

In order to have a smooth frequency output a low-pass filter is used at the output terminal. This ensures a slow change in frequency and thereby prevents oscillations in the system. The desired frequency is used as an input to a three-phase sine generator which generates the phase voltages used as reference for the controlled sources. The amplitude and phase angle are set constant in this thesis and found by use of the load flow tool explained in Section 4.3.

Chapter 6

Simulations, Results and Discussion

In this chapter three different aspects within this system will be tested and discussed. First the control concept of varying the frequency will be tested, and the effect of changing the frequency instead of keeping it constant will be presented. The second aspect that will be studied is the effect of changing the voltage level for the transmission cable when the wind farm is operating below rated effect. The third and last aspect is how the losses and the reactive power flow can be minimized by using an active compensation.

6.1 Variable Frequency

The control concept presented in Section 5.2 will now be tested. In the two first cases both turbines are exposed to the same wind speed. The wind speed is not based on any real measurements, but chosen to effectively test the different elements of the control concept like a decreasing and increasing wind speed as well as operating at different levels. In order to study the effect of using a variable frequency system the results will be compared to a case where the frequency were kept constant despite the wind changes. In the third case the NOWITECH turbine will be exposed to a different wind speed than the aggregated wind park turbine.

6.1.1 Case 1 - Variable Frequency

The results from the frequency control is presented in Figure 6.1. At $t = 20$ s the wind is slowly decreasing from 13 m/s to 9 m/s. Here the controlled frequency, referred to as simulated in the figure, is operating above the optimal frequency. The optimal frequency is based on MPPT calculations where the wind speed is

known. This result is exactly as expected. The control system is slowly regulating the frequency, and hence the speed, as the wind speed goes down. Another reason for the controlled frequency to be lagging the optimal frequency is due to the fact that the speed of the generator is decreasing. Slowing down the generator speed implies taking out more power than in the wind alone. Therefore the control system will experience more generated power than the wind energy provides.

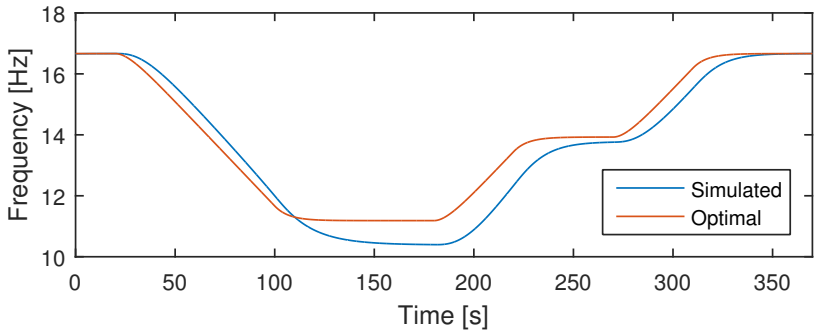

Figure 6.1: The simulated frequency versus the optimal frequency.

When $t = 100$ s the wind speed stabilizes at 9 m/s. A problem that now occurs is that the controlled frequency is stabilizing at a lower level than the optimal frequency. This problem can be explained by looking at the how the losses in the transmission is changing when both the power produced and the frequency is changing. The losses is shown in Appendix C.1 in Figure C.1. As explained in Section 5.2 the frequency versus power curve that is used to control the frequency is based on the power loss when operating at maximum. Since the total losses varies during operation at different levels the control system should take this into consideration. Then as a result of not doing this, the control system will choose a different frequency than the optimal. To further develop the lookup table and include the different losses at the different levels should be done, but was left out due to the time consuming process.

At $t = 180$ s the wind speed starts to increase up to 11 m/s. As expected this results in an increased energy produced at the wind farm and hence the control system starts to increase the frequency as well. When the wind is stabilizing at 11 m/s at $t = 220$ s the frequency will also stabilize itself. It is now seen that the offset between the optimal frequency and the frequency found by the control system is smaller than at lower level with a wind speed of 9 m/s. This is due to the power losses now being closer to the losses at maximum operation and hence a smaller deviation to the actually power delivered to the grid is obtained. When the wind speed ramps up to the rated value of 13 m/s the control system finds the optimal frequency. A scatter plot showing how the wind turbines operates along

the C_p-curve is presented in Appendix C.1 in Figure C.2. The figure shows that the control system is not able to operate at the optimal point during the whole simulation as already highlighted.

The issue with the lookup table not being optimized for the variations in power loss can be shown in Figure 6.2. The reference signal is the input for the frequency control and it is clearly not following the simulated signal which is the power input at the turbines. If the actual losses where included in the reference signal the two lines would be equal and then as a result of this they would comply with the optimal line.

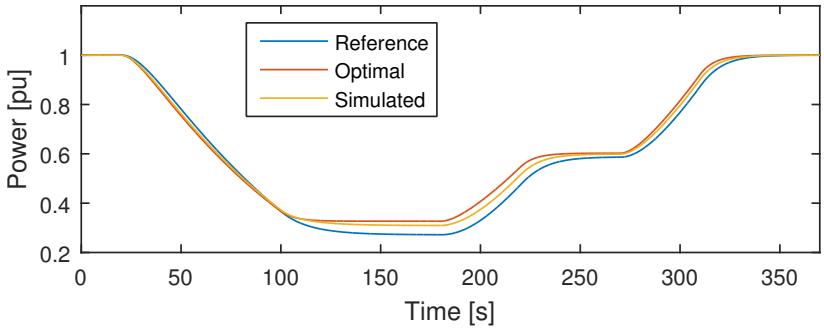

Figure 6.2: The optimal power curve, the input power reference signal for the frequency control and the simulated power input to the turbines.

Instead of optimizing the lookup table further more the results could possibly be improved by doing some other changes in the system that will affect the reactive power flow in the system. As the reactive power exchange with the grid is not controlled the system draws a considerably amount of reactive power from the grid which will result in higher losses in the system. As already mentioned in Section 4.2.4, when referring to the grid, it is actually the converter terminals that is intended. Figure 6.3 shows the active and reactive power measured at the generator side converter terminals.

The shunt reactors in the system is set at a fixed value as explained in Section 4.2.3. They serve to compensate for the reactive power generated in the cable. However, when the frequency is changed a new challenge occurs due to the components dependency on the frequency. The reactive power generated in cable will be lower when the frequency is lowered, while the reactive power compensated for in the shunt reactors will increase. Hence the change in frequency will have to be considered when designing the shunt reactors in order to reduce reactive power flow and losses. More about measures to do this in the following sections.

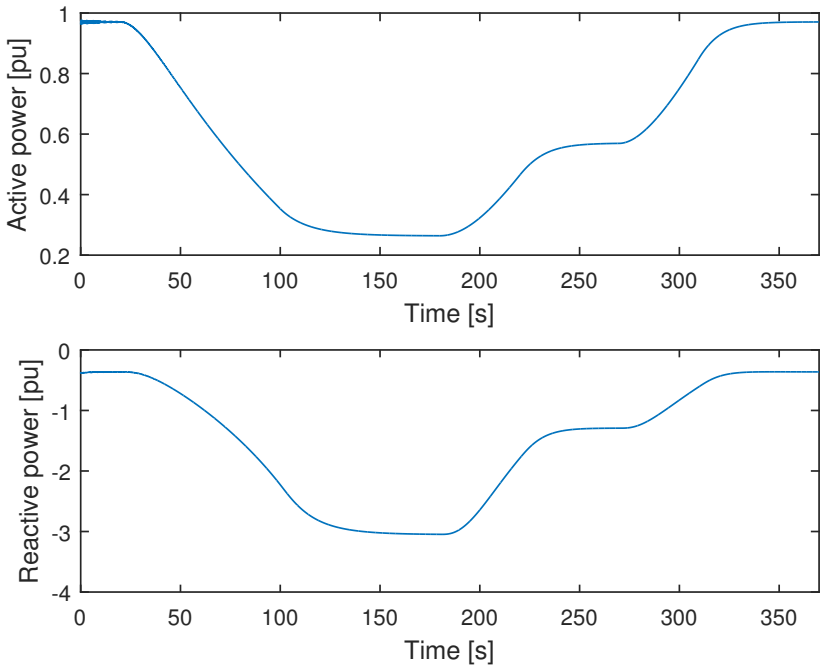

Figure 6.3: Active and reactive power delivered at the generator side terminal of the converter when the system uses a variable frequency.

6.1.2 Case 2 - Constant Frequency

Through simulations the proposed system that is modelled have proven to not be able to operate under the same wind speed range that the turbine alone would be. When the wind speed reaches 8 m/s the system is no longer able to deliver power to the grid the way it is modelled. By controlling the reactive power flow, and optimizing the system for such low frequency's that these low wind speeds implies might make the system able to deliver power at even lower wind speeds. However, to further increase the wind speed range has not been the focus in this thesis. Therefore it was found interesting to look at how necessary the frequency control actually would be. As the wind speed range is smaller, the effect of not operating at the maximum operation point might not be that severe. The same wind speed as used in case 1 was therefore subjected to the system, but now the frequency was kept constant, equal to 16 $\frac{2}{3}$ Hz.

The results presented in Figure 6.4 shows how the reactive power exchange with the grid have a positive development. It is not reaching high unacceptable values and might therefore not be that important anymore. Figure C.3 in Appendix C.2 shows that the losses in the system is decreasing when the wind speed, and

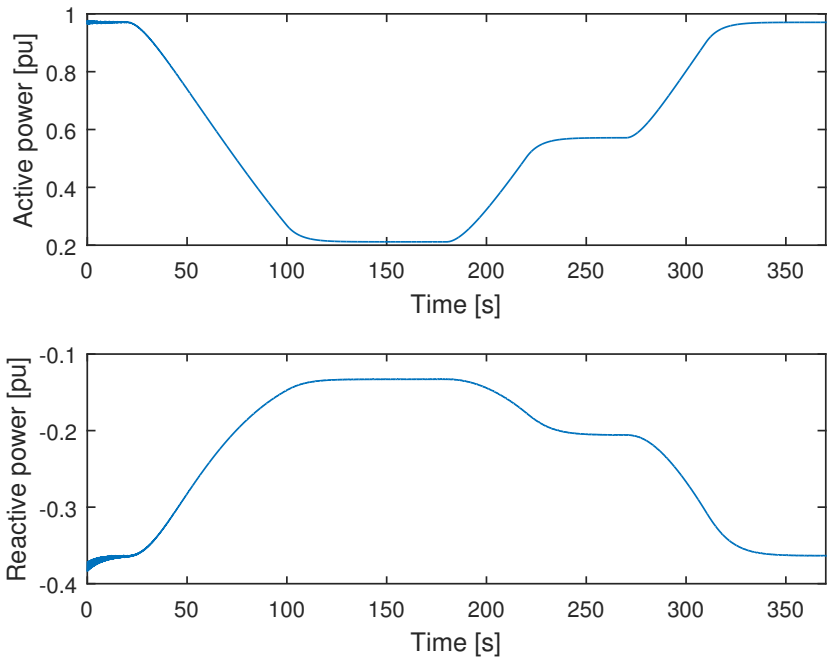

Figure 6.4: Active and reactive power delivered at the generator side terminal of the converter when the frequency is kept constant.

thereby the reactive power drawn from the grid, decreases. So by not changing the frequency the requirements for the reactive power control and compensation will be smaller. However, the active power delivered to the grid is of course smaller as well. The losses in active power would mean economic losses for the operator. It would therefore also be of interest to look into how big this loss would be. In Figure 6.5 the active power delivered to the grid for both the variable frequency system and constant frequency system are presented. The lower the wind speeds are, the less optimal would it be to keep the frequency constant. This can be shown from the power graphs presented in Section 3.2, Figure 3.14. However, as the control system in this thesis is not perfectly optimal this negative effect is only present for the lowest wind speed. For the scenarios were there are an increase in wind speed it can be shown that keeping a higher frequency than optimal is an advantage compared to the variable frequency system. This is a result of the slow frequency regulation in the variable frequency system which results in a loss in possible production. Keeping a higher frequency allows the system to respond faster to the increased wind speed. The results is that the constant frequency system is able to produce more active power in this scenario. In Figure C.4 in

Appendix C.2 it can be shown how far off the optimal operation point the system operates when the system frequency is kept constant. Overall the results from the comparison between the two different techniques shows how important an efficient and accurate control system would be.

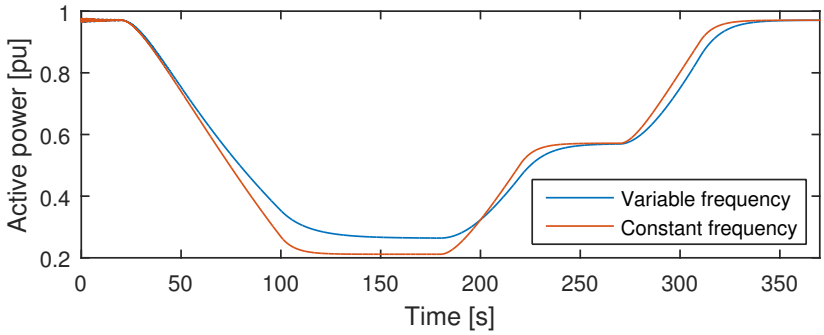

Figure 6.5: Active power delivered at the generator side terminal of the converter for both variable frequency and constant frequency.

6.1.3 Case 3 - Different Wind Speeds

The main reason for having one converter in each turbine like most of the turbines have today, is that the turbines will seldom experience the same wind speed, and hence they will have different optimal speed. Usually the turbines would be able to control the rotational speed independently of the others. Therefore it is of great interest to have further look into how the control system will work when different wind speeds are applied to the turbines. The wind speeds applied to the turbines can be found in Appendix B.2. The frequency control results from the simulation are shown in Figure 6.6.

From this figure it is shown that the frequency is controlled in a way that follows the aggregated wind turbines optimal frequency as this would result in the most power generated. This is exactly as expected and the positive effect of this can be seen in Figure 6.7 where the generated power in each turbine is compared with the optimal. It is obviously an advantage having the 190 MW turbine operating closer to its optimal operation point than the 10 MW turbine. A scatter plot showing the operation points for the turbines during the simulations is presented in Figure C.5 in Appendix C.3.

The amount of power being spilled when the wind turbines cannot operate at the optimal operation point is of great interest when looking at the economic aspect. From the simulations it is actually possible to calculate how big this loss would be. However, there is one important aspect, that is not simulated, but might be a relevant scenario in a real wind farm. That is, dependent on the placement of the

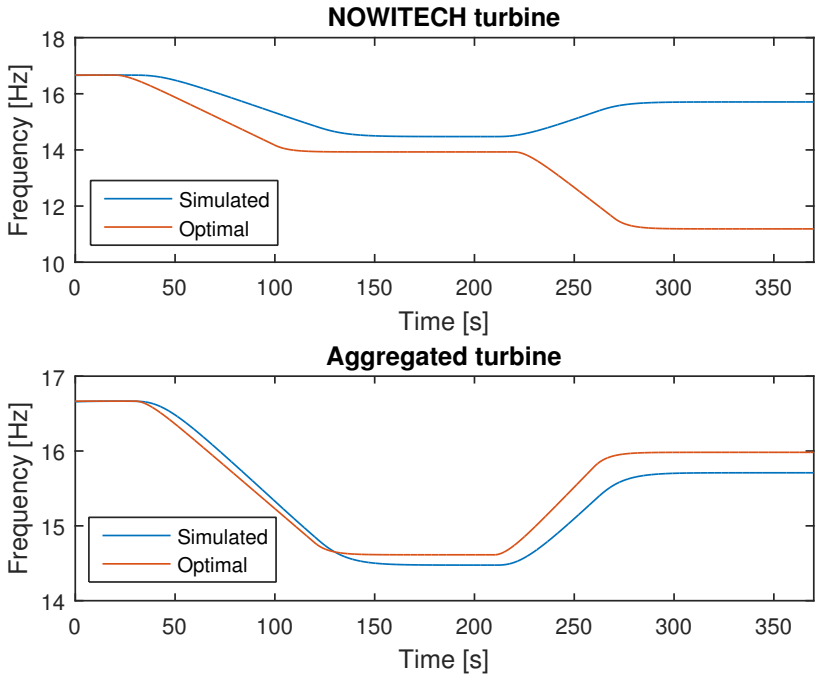

Figure 6.6: The system frequency versus the optimal frequency for the turbines during different wind speeds.

turbines, the loss of power at one turbine might be gained at another wind turbine. In an offshore wind farm the turbines are usually spread out on a quadratic or rectangular area. Therefore, the wind power that passes the turbines at the edge of the wind farm would hit the turbines behind them. In that way the power being spilled in one turbine might be gained in another one. Simulation of this requires a totally different software and model and it has therefore not been studied. It is therefore recommended to further investigate the effect of this when looking at the economic aspect.

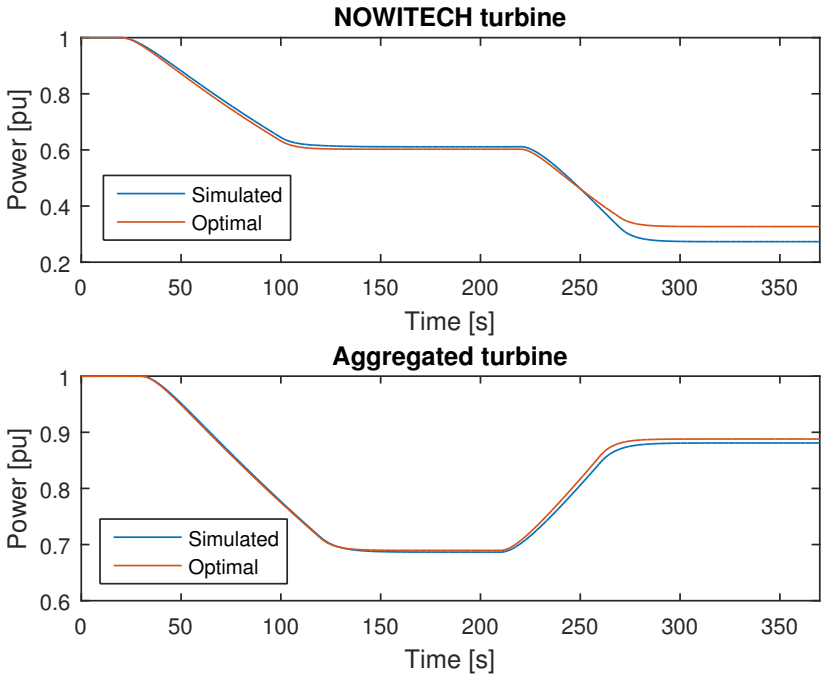

Figure 6.7: The generated power versus the optimal power for the turbines during different wind speeds.

6.2 Variable Transmission Voltage

The idea of changing the transmission voltage in order to minimize losses as presented in Section 3.8 will now be tested. If the wind speed is just 11 m/s, only 2 m/s under the wind parks rated wind speed, the wind park will only be able to produce around 0.6 of its rated power capability. From the graphs presented in Figure 3.28 it is shown that the cable efficiency will be reduced when the transmitted power reduces. Based on these graphs, a power production of around 0.6 pu or 120 MW should be transmitted through a cable of 0.8 pu or 176 kV in order to achieve maximum efficiency. The system is therefore initialized with 0.6 pu power production and a transmission voltage of 176 kV. In the first case the wind speed is kept constant, 11 m/s, and the total losses from the generator output to the onshore converter terminal is measured. In the second case the wind speed will vary from 11 m/s to 9 m/s. At a wind speed of 9 m/s the wind park will have power production of 0.33 pu or 66 MW. In both cases the results will be compared to the system with a transmission voltage of 220 kV.

6.2.1 Case 1 - Reduced Transmission Voltage under Constant Wind Speed

By lowering the transmission voltage the active effect delivered to the grid increased as shown in Figure 6.8. Another benefit is that the reactive effect drawn from the grid is lower for the 176 kV transmission system. However, the reactive effect is still too high and measures needs to be done in order to control this. One important thing to mention is that the shunt reactors have not been changed and are therefore still optimized for the system running at rated frequency. Therefore these results enhances the necessity of having an active compensation.

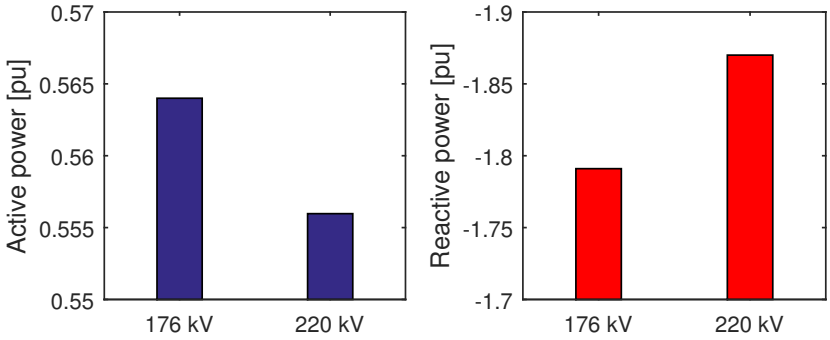

Figure 6.8: Total active and reactive power delivered to the grid for the systems with different transmission voltage level.

As a result of the reduced losses and that the control system is not perfectly optimized, as highlighted in the previous section, the system is actually able to produce more active power. The produced power and the received power for both systems is shown in Figure 6.9. In this model there is obviously an advantage of using the 176 kV voltage level for operation at lower wind speeds. When subtracting the delivered power from the produced power the losses is found to be 9.29 % smaller for the 176 kV system compared to the original system. The total losses for both systems can be shown in Appendix C.4 in Figure C.6.

6.2.2 Case 2 - Reduced Transmission Voltage under Variable Wind Speed

Minimizing losses becomes even more important when the wind farm is operating at even lower levels of power production. When the wind speed is only 9.5 m/s the wind farm is capable of producing 66 MW. The results presented in Figure 6.10 shows that the 176 kV transmission system will deliver more active power to the grid. It will also draw less reactive power from the grid. Comparing the losses for the two different systems there is an improvement of 10.79% for the lowest level

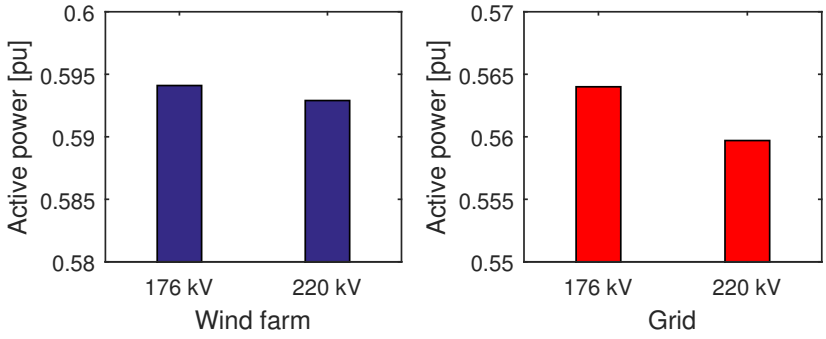

Figure 6.9: Total active power produced at the wind farm and delivered to the grid for the systems with different transmission voltage level.

of power production compared to the 220 kV system as seen from Figure C.7 in Appendix C.4. This is obviously an advantage as it might make the system able to operate at even lower power levels before it has to shut down production.

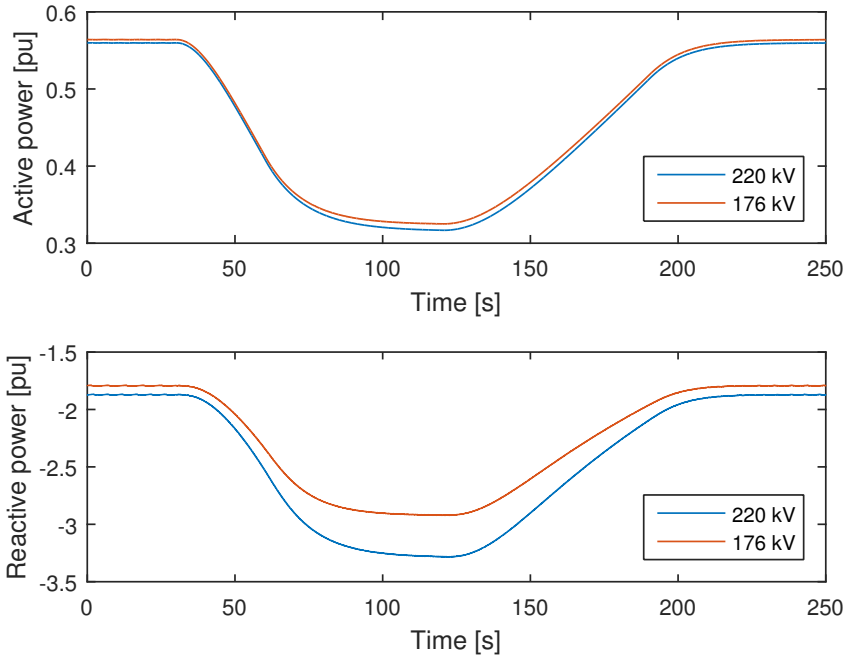

Figure 6.10: Total active and reactive power delivered to the grid for the systems with different transmission voltage level during a variable wind speed.

6.3 Compensation

Based on theory in Section 3.9 and previous results the necessity for some sort of compensation is definitely present. In this section the effect of using an active compensation will be presented. However, as implementation of an active shunt reactor that continually changes the reactive compensation level based on the frequency proved to be difficult, the shunt reactors inductances will be manually changed for the different levels in the first case. In the last cases the shunt reactors will be disconnected by use of switches during the simulations. For the final case a capacitor bank is also introduced to the system as the results will prove the necessity of reactive power supply at the generator terminals.

6.3.1 Case 1 - Reduced Compensation under Constant Wind Speed

The first case extends the first case in Section 6.2 where the wind speed was set to 11 m/s resulting in a power production of 0.6 pu or 120 MW. In addition to changing the transmission system voltage level, the shunt reactors are also modified. The inductances are manually changed before initializing the system. In the same way as in Section 4.2.3, the shunt reactors indcutances are first found by calculations and then changed based on the load flow analysis. From calculations the inductances were found to be 9.73 H each, but as a result of the load flow analysis they vere changed to 13.5 H. In Figure 6.11 it can be shown how this further increased the active power delivered to the grid and reduced the reactive power drawn from the grid.

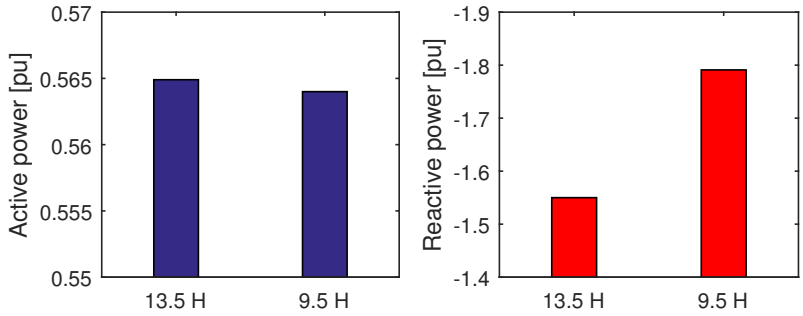

Figure 6.11: Total active and reactive power delivered to the grid for the systems operating with different shunt reactors. The legend shows the inductance value used in the shunt reactors.

This also led to 2.7 % lower losses compared to the case where only the voltage level was changed. The total losses for this case is presented in Figure C.8 in

Appendix C.5.

6.3.2 Case 2 - Active Compensation under Variable Wind Speed

As explained in Section 3.9 the control of compensation should be done based on the necessity of compensation at that time. Instead of implementing such a comprehensive control method a simplification has been made that enables to study the same effect of controlling the compensation during the simulation. The shunt reactors has been connected through a switch which is controlled by a time signal. The time signal was found based on the reactive power drawn from the grid in the main simulation, case 1 in Section 6.1. The time were the switches should open and close were chosen to be when the reactive power was around -2 pu. It should be pointed out that -2 pu is far too high in a real scenario, and that this is just to show the result of changing the compensation, and how the system will react. From Figure 6.3 it was found that the reactive power passed -2 pu at $t = 95$ s which was then chosen as the time to open the switches. The switches were then closed at $t = 215$ s when the reactive power drawn from the grid was once again passing -2 pu, only that is was decreasing in this case. The active and reactive power delivered to the grid from this simulation are presented in Figure 6.12.

The results shows that by turning off the compensation the system still draws a huge amount of reactive power. A further investigation of this shows how the generators start to draw a serious amount of reactive power as the frequency and power production drops. This means that for operations at this level the generators should be connected to a capacitor bank that will supply reactive power when needed. The results also shows why the reactive power compensation should be firmly controlled and not switched off and on at once. The reconnection of the shunt reactors, at $t = 215$ s, causes severe oscillations in the system and from Figure 6.12 it is clearly shown how both the active and reactive power reacts to this sudden change in the system.

Based on the results above, a more realistic way of changing the compensation was tested. Instead of disconnecting and connecting all the compensation at once, it was tested to step-wise reduce and increase the compensation respectively. By dividing the shunt reactors in four inductances with one switch each, at both sides of the cable, this could be achieved. In all this resulted in eight switches, four at each side, where two and two operated together, meaning at the same time signal. This leads to the same compensation at both ends at the same time. The value of the inductances was chosen to be four times the original value as the four inductances then would be equal the original when they are in parallel. The time signal was once again found based on the reactive power drawn from the grid in the main simulation as already explained above. In this case the times were taken when the reactive power was equal to -1.0, -1.5, -2.0 and -2.5 pu. The results are

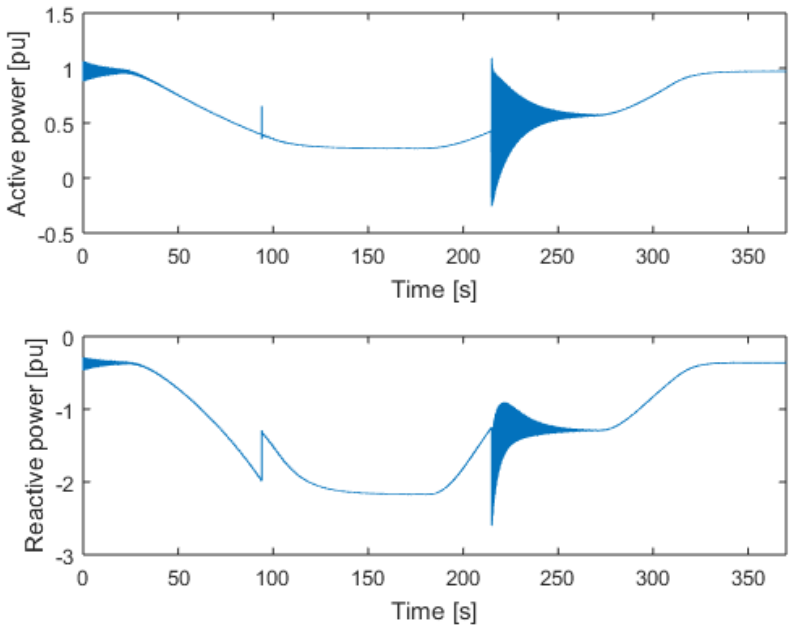

Figure 6.12: Total active and reactive power delivered to the grid under active compensation.

shown in Figure 6.13. By having smaller changes in the compensation the results shows that the oscillations in the active power becomes smaller in amplitude for the first operation when connecting the shunt reactors to the system again. However, as the system hasn't reached a stable level before the next operation takes place the oscillations due to the following changes becomes even worse. If and even higher number of steps were used, instead of only four steps, these oscillations might be prevented. Overall the reactive power drawn from the grid is reduced compared to the previous case. This shows that there is a positive effect of using an active compensation as assumed. Despite this, the reactive power drawn from the grid is still too high due to the above mentioned problem with the generators consuming reactive power.

What is also noticed in the results in Figure 6.12 and 6.13 is that the oscillations that occurs when reconnecting the shunt reactors are poorly damped. A poorly damped system has several disadvantages and therefore an improvement of this should be carried out. A further investigation of these oscillations reveals that the system is left marginally stable after the sudden disconnection of the shunt reactors. Figure 6.14 shows that there are already some small oscillations in the system before the reconnection. Then when the shunt reactors are reconnected

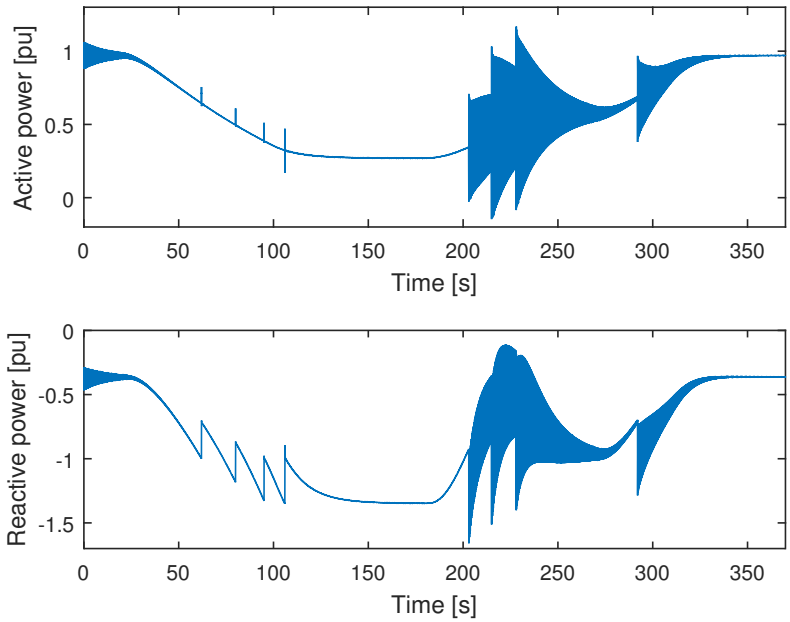

Figure 6.13: Total active and reactive power delivered to the grid under active compensation with several steps.

these oscillations becomes even larger in amplitude. The origin of the oscillations seems to be the system frequency as the frequency of them are found to be the same as the system frequency at that time. Due to the frequency control the frequency at the time is around 12 Hz. In order to verify this the same simulation were done without frequency control, instead the frequency were kept constant equal to 16 $\frac{2}{3}$ Hz. The result from this simulations, shown in Figure 6.14, verifies this assumption as the oscillations now has a frequency of around 16 Hz. This may show that running the system at this low frequency is a bigger challenge than expected. Further research of this feature should definitely be done as this could be a serious problem that might prove the system to be infeasible.

6.3.3 Case 3 - Active Compensation under Variable Wind Speed with Capacitor Banks

The necessity of the compensation was found through the load flow analysis done to initialize the system. The model were also in need of these shunt reactors in order to stabilize itself during start-up of the simulations. However, when studying the reactive power flow in the previous cases it is always a problem that the system

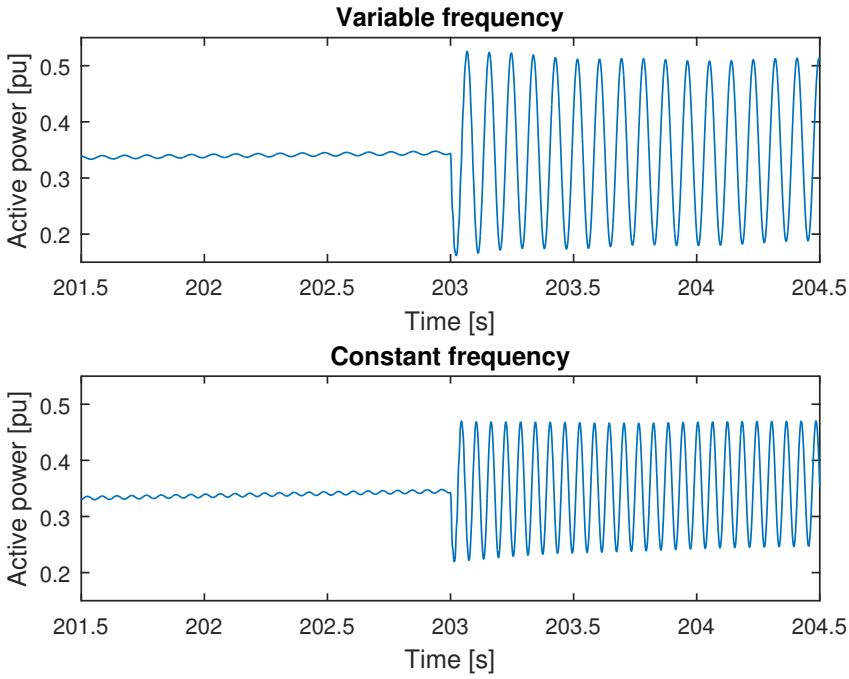

Figure 6.14: Oscillations when reconnecting the shunt reactors.

draws a serious amount of reactive power from the grid. When the wind speed was lowered the shunt reactors were proven to actually aggravate this problem. After disconnecting the shunt reactors it was found out that the generators would need reactive power supply. When the generators are exposed to the frequency change they starts to draw a serious amount of reactive power in order to maintain the active power production at rated voltage level. With no other option this reactive power is supplied by the grid which is not optimal for the transmission system at all. The necessity of capacitor banks at the generator terminals are thereby present.

Therefore this case will also include the connection of two capacitor banks, one at each generator. The capacitor banks are connected by a switch when the reactive power is needed, around -0.5 pu. The same simplification as done for the active compensation has been made, meaning that the capacitor banks are switched fully on or off based on reactive power consumption in previous simulations. As the system is very sensitive to such severe changes it would only be stable for wind speeds down to 10 m/s, and hence the system is only simulated for wind speeds above this level. Or more specific, the system is exposed to a wind speed decreasing from 13 m/s to 10 m/s before going back to 13 m/s again. The shunt reactors was

also changed based on the results, allowing a better control of the reactive power interchange with the grid. The inductance value was increased to twice its size which means that the shunt reactors will compensate for half of the reactive power it originally did. This also means that switching on and off the shunt reactors will result in a smaller change for the system, which should improve the stability in the simulations.

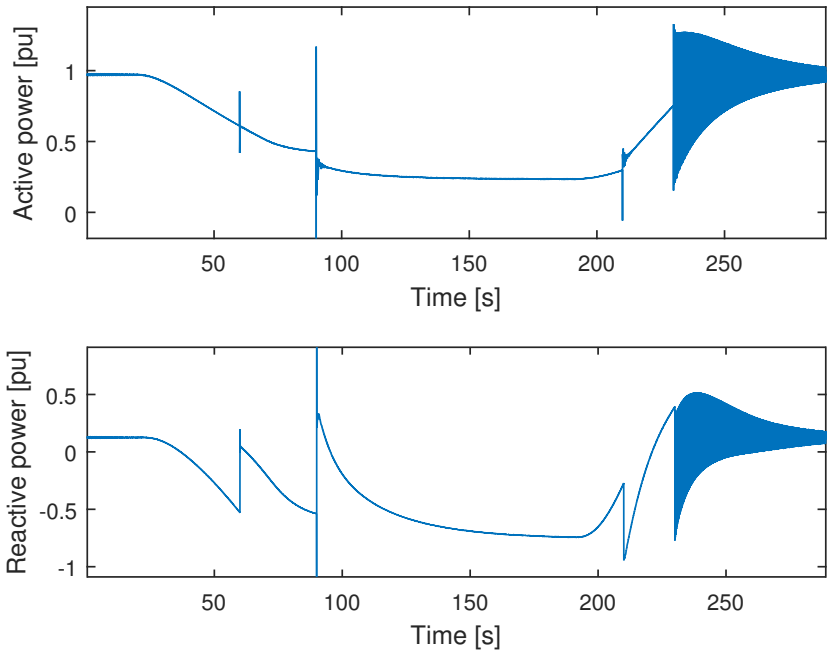

Figure 6.15: Total active and reactive power delivered to the grid when use of active compensation and capacitor banks.

The result is shown in Figure 6.15. At $t = 60$ s the shunt reactors are switched off which results in jump in reactive power exchange with the grid. The system ends up with a small production of reactive power instead of consumption of reactive power. As the frequency is still decreasing the system, or more specific the generators, need more reactive power. Therefore at $t = 90$ s the capacitor banks are switched on which once again results in a jump in reactive power exchange with the grid as expected. It also results in some high oscillations which is not shown in the figure. The oscillations are quickly damped, but has a peak of around 2 pu which is not acceptable. This clearly shows that the changes should be done in smaller steps, by use of FACTS devices for example. It is therefore important to point out that this solution is only done to show the effect of the capacitor bank

and shunt reactor, and that in a real system less brutal techniques would have been applied. Before the wind speed starts to increase around $t = 190$ s the system stabilizes with a reactive power consumption from grid around -0.7 pu. Together with other results from the model it shows that another capacitor bank should have been connected at the generator terminals. At $t = 210$ s the capacitor banks are disconnected and at $t = 230$ s the shunt reactor are connected. The results shows that the first operation should have been done later. However, the impact it would have on the system is still the same, and it shows how the disconnecting of reactive power supply at the generator terminals forces the grid to supply this power.

6.4 Discussion

The proposed wind farm system has been modelled and tested thoroughly. The first thing that was looked into was the control system of the system. Based on the results of this it was found interesting to look further into different measures to reduce losses in the system and minimize reactive power flow in the system. The simulations has been selected in order to highlight the benefits of these measures and to effectively show the necessity of a good control system and FACTS devices. This section will discuss the model and some of the results with respect to possible improvements. It will also highlight some of the challenges that this system faces.

The control systems that control the amount of power input to the generators are working as expected. However, as it consists of some simplifications it won't be suited for wind speeds above rated wind speed. In a more detailed version were the scope is to look at for example fluctuations in wind speed around rated wind speed and its impact on the system the wind turbine power control should be implemented. The NOWITECH reference turbine is originally designed for pitch control of the blades. That is why simplification of limiting the wind speed to the rated wind speed were done in the simulations. By adding the pitch regulator the power output of the control system would be more realistic as it would be delayed due to the slow dynamics in changing the blade angle. This means that in some cases it could actually generate more power than rated as the blades are not pitched out fast enough. Especially when using real wind speed measurements this feature will be important. Anyway, another power control that might be more suited for the system is the stall control. This control method will be discussed more later.

For the frequency control system it has already been pointed out in Section 6.1 that it needs to be further optimized. As mentioned, the reference frequency versus power curve does not take into account that the system losses varies with the different power levels. However, there is also another control concept that might be better in terms of finding the maximum operation point for the wind farm, namely the hill climb search control presented in Section 3.3. As implementation of this control concept failed to work in the simulations and time was limited

it has not been presented. Two of the challenges that was found was that it was operating too slow and causing oscillations in the system. As the system is very sensitive to changes in the frequency the control system should be tuned to carefully change the frequency and avoid oscillations around the optimal frequency. Another solution for the control system could be to use an interaction between the two mentioned technique. At first the system should be controlled based on the theoretical frequency versus power curve. And then when it is stabilized the hill climb search control should take over in order to ensure optimal power generation for the whole wind farm. The optimal operation points are expected to be close to this curve and hence this control technique might be faster than the regular hill climb search control.

It has been shown that changing the transmission voltage level during operations at lower power levels will minimize the losses. This was tested based on the work done in [37] where the same results is found. Minimizing the losses will have a severe impact on the economical aspect. Not only because of the reduction in losses, but also because the system might be able to operate for even lower power levels. Even though the change of voltage level only implies a small change in the cable efficiency it will represent a large reduction in losses. In this system the losses were found to be reduced by 9.29 % when the wind farm was operating at 0.6 pu power production. A further extension of this concept would be to have additional voltage levels allowing continuously optimization of the transmission voltage based on the power production as explained in Section 3.8.

There are still some uncertainty about how the different components in the system will react to the frequency changes and a further study of this is therefore recommended. A lower frequency results in less reactive power production in the cable. The generator on the other hand will start to draw a serious amount of reactive power which should be compensated for by installing capacitor banks at the generator terminals. These results shows the necessity of FACTS devices with a suitable control system. Minimizing the reactive power flow in the system, and especially in the cable, will result in lower losses in the system. It is however interesting to look further into to the generators and their need of reactive power. The result is found to be really high, and therefore some of the problem could be the model itself. Another challenge that was discovered was that the system started to oscillate with a frequency equal to the system frequency when disconnecting and reconnecting the shunt reactors. Whether this is an actual weakness in the system or just a result of the severe and sudden change has not been uncovered. As this could be a serious problem proving the whole system infeasible a further research within this topic is highly recommended.

The proposed system includes several aspects that one does not know the consequences of today. Further investigation of the different aspects needs to be done, and proper solutions to the different challenges must be developed. The incentive

for pursuing this system is the cost saving. The use of LFAC transmission system has already been proven to be a cost effective solution [5]. By combining it with the slimmed turbine concept the solution is expected to be even more cost competitive as one reduces several expensive components. However, as the results have shown there are challenges that might add other components to the system. In Section 2.2 the transformers has been brought up as the component that will be the most affected one. The necessary increase of the transformer size will increase the costs as well, and it also might affect the construction of the turbines.

One major disadvantage with the proposed system is the lack of controllability. By not being able to operate each wind turbine at its optimal operation point means that potential generated power is lost. However, as mentioned in Section 6.1, this might not be that much as first assumed as the lost wind power might be gained by another turbine. The placement of the turbines are therefore of great interest as it could possibly prevent some of these losses. A further study of this is therefore recommended. Another problem that may occur with this type of system, which should be further investigated, is how the synchronous operating wind farm will affect the mechanical stresses on the wind turbines. When the turbines are forced to operate at the same rotational speed even though not being exposed to the same wind speed there are forces that will work against the wind if the wind speed is higher at that turbine. By pitching the blades this will to some extent be prevented, given that the pitch control implemented also is able to act even though the wind speed and the rotational speed is not at rated level. This involves a further extension of the regular pitch control. However, pitching the blades are not done immediately and this problem may lead to additional stress on the turbines. Adding extra stress to the wind turbines will shorten their lifetime making the system less attractive as it reduces the potential revenues. It could also result in an instability in the system if the wind forces overcome the electrical forces. Therefore, the use of stall control might be a better solution as already mentioned. By stalling the turbines the wind forces acting on the turbine in the rotational direction will decrease. This eliminate the use of pitch control and the advanced control strategy it would need. If stall control is used, the control strategy onshore should be updated. The power curve of a stall controlled turbine will have a drop after it has reached rated power production if the wind speed keeps increasing. If the frequency control is still active this means it will start to reduce the speed even though the wind speed is above rated value. Therefore the frequency control based on the power measurement should only be active until the wind farm has reached rated power production. Then the frequency is fixed and the stall control will ensure operation at the rated level. The frequency control shouldn't be reconnected before the power production reaches a lower value than under stall control, meaning that the wind speed has dropped and controlling the frequency will therefore be beneficial.

The model also contains some elements with a potential for improvements. The values for the transformers are not accurate and exclusively based on standards from MATLAB Simulink with no empirical testing. The same applies for the generator which is actually supposed to be a PMSG. Based on scope this thesis it was not found important to change the generator. The cable parameters, which are based on a datasheet for ABBs submarine cables, will not need any changes as long as the rated power level stays the same. Overall, the model works as expected and should serve as a base for further studies. It should however be mentioned that simulating a large model like this with such a small time-step in MATLAB SimPowerSystems is very time-consuming. If one also wish to save the data from the scopes to the workspace it demands a good computer with a large memory.

Chapter 7

Conclusion

A proposed wind farm system using a slimmed turbine concept combined with low frequency AC transmission to shore have been modeled in order to investigate if it represents a feasible way of designing an offshore wind power system in the future. This thesis must be looked at as a preliminary study where a model of the system was made and some challenges were approached. Further investigations and a more detailed study of the different elements are recommended. This section presents the most important conclusions that have been drawn.

The control system that were chosen is based on the power signal feedback technique, whereas in stead the frequency, and hence the speed, is decided based on active power measurement at the grid terminals. The model of this has some points for improvements. Obtaining the correct frequency versus power curve is found to be difficult and time-consuming. The option of using the hill climb search control or a combination of both of them should be tested. Combining both of them requires a less precise reference curve, and it might respond faster to wind speed changes than the hill climb search control alone.

When the wind turbines are exposed to different wind speeds the system proves that it will lose some of the power it could have generated due to the lack of controllability. It is however difficult to calculate exactly how much this would be in a real scenario. Especially since it is possible that some of the lost power at one turbine could be gained at another one.

The cable efficiency can be increased by using tap-changers to adjust the operating voltage based on the power generation. The system proved a reduction in losses of 9.29 % for an operation at 0.6 pu power production when operating with an transmission voltage level of 0.8 pu. Minimizing losses will increase the feasible wind speed range the system will be able to operate under.

The results showed that the reactive power flow in the system is clearly dependent on the frequency as expected. It is therefore concluded that implementation

of FACTS devices are needed and a suitable control of these have to be developed. The generators severe reactive power demand are found highly interesting and further research are recommended to confirm or reject this result.

Chapter 8

Further Work

This thesis must be viewed as a preliminary study where the goal was to establish a working model of the proposed system and investigate some of the electrical aspects that are found interesting. This section contains some topics that it is encouraged to perform further research on.

8.1 Improve frequency control system and implement hill climb search control

A challenge in the control system used in this thesis is that it will be difficult and time-consuming to find the optimal frequency versus power curve used as a reference for the control system. This is due to the fact that the losses in the system are not constant when the frequency varies. By either switching to the hill climb search control presented in Section 3.3 or implement a combination of them would increase the efficiency as it ensures operation at the maximum operation point for the wind farm. Another improvement that would also be necessary if the stall control concept is used is to implement the effect of this in the control system onshore.

8.2 Improve reactive power compensation.

Operating a large system with a varying frequency has been proven to have severe impact on the reactive power flow in the system. It is therefore necessary to implement a thyristor controlled capacitor bank at the generator terminals and thyristor controlled shunt reactors at the cable ends. The control concept of these will be important in the goal of reducing reactive power flow in the system, and hence minimize the losses in the system.

8.3 Update the modelled system

Further work should also include updating some parts of the modelled system. The generators are based on standard values found in MATLAB Simulink and should therefore be updated to be a more representative for the reference turbine. It is also modelled as synchronous machine with constant internal voltage instead of a PMSG. Based on what the scope of the further research is, changing the generator may be necessary. Another part of the modelled system that has not been prioritized are the transformers. They are also based on standards found in the Simulink library. As this system would require a change in the physical size of the transformer compared to the regular 50 Hz transformer it may impact some of the parameters in the model. However, this has not been considered to have a big impact on the results.

8.4 Other suggestions for further work

As this is an entirely new way of designing an offshore wind power system it is of course several other things that should be further investigated, both in terms of electrical aspects, economical aspects and mechanical aspects.

In terms of the electrical aspects it is important to dig deeper into which harmonics will occur in the system and the impact of them. It is also of great interest to test the system for different fault scenarios and find the best suited protection strategy. The oscillations found in Section 6.3.2 with a frequency equal to the system frequency should also be investigated in further work with the system.

Bibliography

[1] European Wind Energy Association. Wind in power: 2014 European statistics. 2015.

[2] H. H. Larsen and L. S. Petersen. Wind Energy - Drivers and Barriers for Higher Shares of Wind in the Global Power Generation Mix. Technical report, Technical University of Denmark, 2014.

[3] P. Bresesti, R. L. Hendriks, R. Vailati and W. L. Kling. HVDC Connection of Offshore Wind Farms to the Transmission System. *Energy Conversion, IEEE Transactions on*, 22(1):37–43, 2007.

[4] M. Björk. Use of Low Frequency Alternating Current for Offshore Wind Farms - Wind Turbine Implications. Technical report, Scandinavian Wind, 2014.

[5] N. Qin, S. You, V. Akhmatov and Z. Xu. Offshore wind farm connection with low frequency AC transmission technology. In *Power Energy Society General Meeting, 2009. PES '09. IEEE*, pages 1–8, 2009.

[6] I. Erlich, R. Braun and W. Fischer. Low frequency high voltage offshore grid for transmission of renewable power. In *2012 3rd IEEE PES Innovative Smart Grid Technologies Europe (ISGT Europe)*, pages 1–6, 2012.

[7] P.B. Wyllie, Y. Tang, L. Ran, T. Yang, and J. Yu. Low Frequency AC Transmission - Elements of a Design for Wind Farm Connection. In *AC and DC Power Transmission, 11th IET International Conference on*, pages 1–5, Feb 2015.

[8] T. Ackermann. *Wind Power in Power Systems*. John Wiley & Sons, Ltd, 2nd edition, 2012.

[9] D. Campos-Gaona, E. Moreno-Goytia, G. Adam and O. Anaya-Lara. *Offshore Wind Energy Generation: Control, Protection, and Integration to Electrical Systems*. John Wiley & Sons, Ltd, 2014.

[10] M. Manohara and S. Sonia. Design of Low-frequency AC Transmission System for Offshore Wind Farms. *International Journal of Emerging Technology and Advanced Engineering*, 2014.

[11] Dr. Terence O'Donnell Dr. Ronan Meere and Mr. Jonathan Ruddy. Comparison of VSC- HVDC with Low Frequency AC for Offshore Wind Farm Design and Interconnection. *EERA DeepWind*, 2015.

[12] Atle Rygg Årdal. Feasibility Studies on Integrating Offshore Wind Power with Oil Platforms. Master's thesis, Norwegian University of Science and Technology, 2011.

[13] T. Haileselassie. *Control, Dynamics and Operation of Multi-terminal VSC-HVDC Transmission Systems*. PhD thesis, Norwegian University of Science and Technology, 2012.

[14] N. Mohan, T. M. Undeland and W. P. Robbins. *Power Electronics - Converters, Applications and Design*. John Wiley & Sons, Inc., 2003.

[15] D. O. Neacsu. Space vector modulation – an introduction. In *The 27th Annual Conference of the IEEE Industrial Electronics Society*, pages 1583–1592, 2001.

[16] A. Yazdani and R. Iravani. *Voltage-Sourced Converters in Power Systems: Modeling, Control and Applications*. John Wiley & Sons, Inc., 2010.

[17] A. Chandra, B. S. Sabha, C. Jain, K. Al-Haddad, R. Arya and S. Goel. Application of voltage source converter for power quality improvement. In *Systems Thinking Approach for Social Problems: Proceedings of 37th National Systems Conference*, pages 335–346, 2013.

[18] D. Retzmann, H. Huang and J. Dorn. A new Multilevel Voltage-Sourced Converter Topology for HVDC Applications. *Cigré Session, B4-304*, 2008, Paris, France.

[19] K. Friedrich. Modern hvdc plus application of vsc in modular multilevel converter topology. In *2010 IEEE International Symposium on Industrial Electronics*, pages 3807–3810, 2010.

[20] Kristin Malene Høvik. Control of Offshore Passive Platform System Voltage and Frequency through Control of Onshore Back-to-Back Voltage Source Converters . Master's thesis, Norwegian University of Science and Technology, 2011.

[21] OpenElectrical. Dq0 Transform. *http://www.openelectrical.org/wiki/index.php?title=Dq0_-Transform*, 2015.

[22] N. Mohan. *Advanced Electric Drives; Analysis, Control, and Modeling, Using MATLAB/Simulink*. John Wiley & Sons, Inc., 2014.

[23] H. Dharmawardena. Modelling Wind Farm with Frequency Response for Power System Dynamics. Master's thesis, Norwegian University of Science and Technology, 2015.

[24] L. Sbita, M. B. Hamed and O. Elbeji. PMSG Wind Energy Conversion System Modeling and Control. *International Journal of Modern Nonlinear Theory and Application*, 2014.

[25] L. Chang and Q. Wang. An intelligent maximum power extraction algorithm for inverter-based variable speed wind turbine systems. *IEEE Transactions on Power Electronics*, 19(5):1242–1249, 2004.

[26] H. Goto, H. J. Guo, O. Ichinokura and S. M. R. Kazmi. Review and critical analysis of the research papers published till date on maximum power point tracking in wind energy conversion system. In *2010 IEEE Energy Conversion Congress and Exposition*, pages 4075–4082, 2010.

[27] G. Putrus and M. Narayana. Optimal control of wind turbine using neural networks. In *Universities Power Engineering Conference (UPEC), 2010 45th International*, pages 1–5, 2010.

[28] A. H. M. Yatim, C. W. Tan, M. A. Abdullah and R. Saidur. A review of maximum power point tracking algorithms for wind energy systems. *Renewable and Sustainable Energy Reviews*, 16(5):3220 – 3227, 2012.

[29] C. Zhao, G. Li, M. Yin and M. Zhou. Modeling of the Wind Turbine with a Permanent Magnet Synchronous Generator for Integration. In *Power Engineering Society General Meeting, 2007. IEEE*, pages 1–6, 2007.

[30] J. C. Burgos, M. Chinchilla and S. Arnaltes. Control of permanent-magnet generators applied to variable-speed wind-energy systems connected to the grid. *IEEE Transactions on Energy Conversion*, 21(1):130–135, 2006.

[31] C. Zhao, G. Li, M. Yin and M. Zhou. Modeling of the wind turbine with a permanent magnet synchronous generator for integration. In *Power Engineering Society General Meeting, 2007. IEEE*, pages 1–6, 2007.

[32] Maria Oana Mora. Sensorless vector control of PMSG for wind turbine applications. Master's thesis, Aalborg University, 2009.

[33] H. Nian, J. Li, J. Liu and R. Zeng. Sensorless control of pmsg for wind turbines based on the on-line parameter identification. In *Electrical Machines and Systems, 2009. ICEMS 2009. International Conference on*, pages 1–6, 2009.

[34] M. Molinas, T. Haileselassie and T. Undeland. Multi-Terminal VSC-HVDC System for Integration of Offshore Wind Farms and Green Electrification of Platforms in the North Sea. In *Nordic Workshop on Power and Industrial Electronics*, 2008.

[35] H. Saadat. *Power System Analysis*. The McGraw-Hill Companies Inc., 1999.

[36] BRUGG Cables. High Voltage XLPE Cable Systems - Techincal User Guide. http://nepa-ru.com/brugg_files/02_hv_cable_xlpe/03_web_xlpe_guide_en.pdf, 2006.

[37] B. Gustavsen and O. Mo. Variable Transmission Voltage for Loss Minimization in Long Offshore Wind Farm AC Export Cables. *ArXiv e-prints*, 2016.

[38] F. F. Silva and C. L. Bak. *Electromagnetic Transients in Power Cables*. Springer, 2nd edition, 2013.

[39] A. F. Sarabia and C. A. Espallargas. Assessment of 42 km, 150 kV AC submarine cable at the Horns Rev 2 HVAC wind farm. Technical report, Department of Energy Technology, Aalborg University, 2010.

[40] J. R. Bumby, J. Machowski and J. W. Bialek. *Power System Dynamics Stability and control*. John Wiley & Sons Ltd, 2012.

[41] Henrik Kirkeby. Control of VSC During Unsymmetrical AC Faults in Offshore Wind Farms. Master's thesis, Norwegian University of Science and Technology, 2013.

[42] S. J. Chapman . *Electric Machinery Fundamentals*. The McGraw-Hill Companies Inc., 5th edition, 2012.

[43] ABB. XLPE Submarine Cable Systems. https://library.e.abb.com/public/2fb0094306e8975c125777c00334767/XLPE%20Submarine%20Cable%20Systems%202GM5007%20rev%205.pdf, 2015.

[44] Z. Zhiling, Y. Shulian and F. Xiang. Using Powergui Capabilities of Matlab in Teaching of Electric Power Engineering. In *Electronic Measurement and Instruments, 2007. ICEMI '07. 8th International Conference on*, pages 3–683–3–686, 2007.

[45] NOWITECH. *https://www.sintef.no/projectweb/nowitech/background/*, 2015.

[46] L. Frøyd, O. G. Dahlhaug, P. A. Berthelsen, S. S. Gjerde T. Kvamsdal et. al. Specification of the NOWITECH 10 MW Reference Wind Turbine. 2012.

[47] K. O. Merz. Pitch Actuator and Generator Models for Wind Turbine Control System Studies. Technical report, SINTEF Energy Research, 2015.

Appendix A

Theory

A.1 Park Transformation

The Park transformation, or direct-quadrature-zero (dq0) transformation, is a mathematical transformation which rotates the stationary three phase coordinate system (abc) [21]. The transformation can be done either as power invariant, like the one presented below, or voltage invariant.

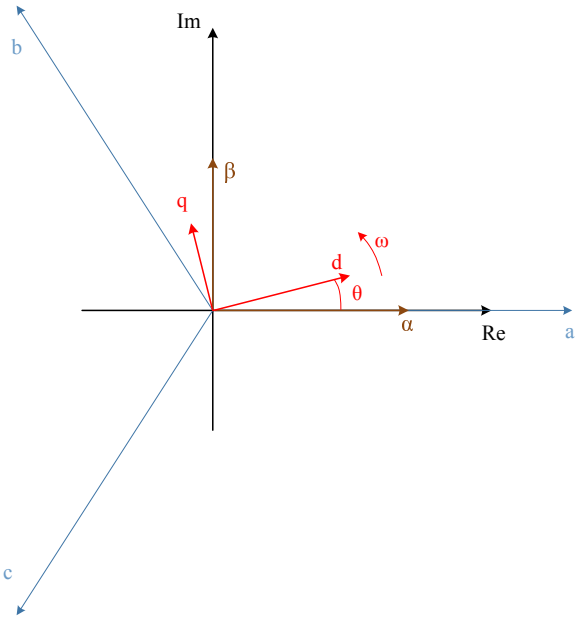

Figure A.1: Relation between three-phase-, $\alpha\beta$- and dq-reference frame.

$$x_{dq0} = \sqrt{\frac{2}{3}} \begin{bmatrix} cos(\theta) & cos(\theta - \frac{2\pi}{3}) & cos(\theta + \frac{2\pi}{3}) \\ -sin(\theta) & -sin(\theta - \frac{2\pi}{3}) & -sin(\theta + \frac{2\pi}{3}) \\ \frac{1}{\sqrt{2}} & \frac{1}{\sqrt{2}} & \frac{1}{\sqrt{2}} \end{bmatrix} \cdot \begin{bmatrix} x_a \\ x_b \\ x_c \end{bmatrix} \tag{A.1}$$

$$x_{abc} = \sqrt{\frac{2}{3}} \begin{bmatrix} cos(\theta) & -sin(\theta) & \frac{1}{\sqrt{2}} \\ cos(\theta - \frac{2\pi}{3}) & -sin(\theta - \frac{2\pi}{3}) & \frac{1}{\sqrt{2}} \\ cos(\theta + \frac{2\pi}{3}) & -sin(\theta + \frac{2\pi}{3}) & \frac{1}{\sqrt{2}} \end{bmatrix} \cdot \begin{bmatrix} x_d \\ x_q \\ x_0 \end{bmatrix} \tag{A.2}$$

A.2 Compensation

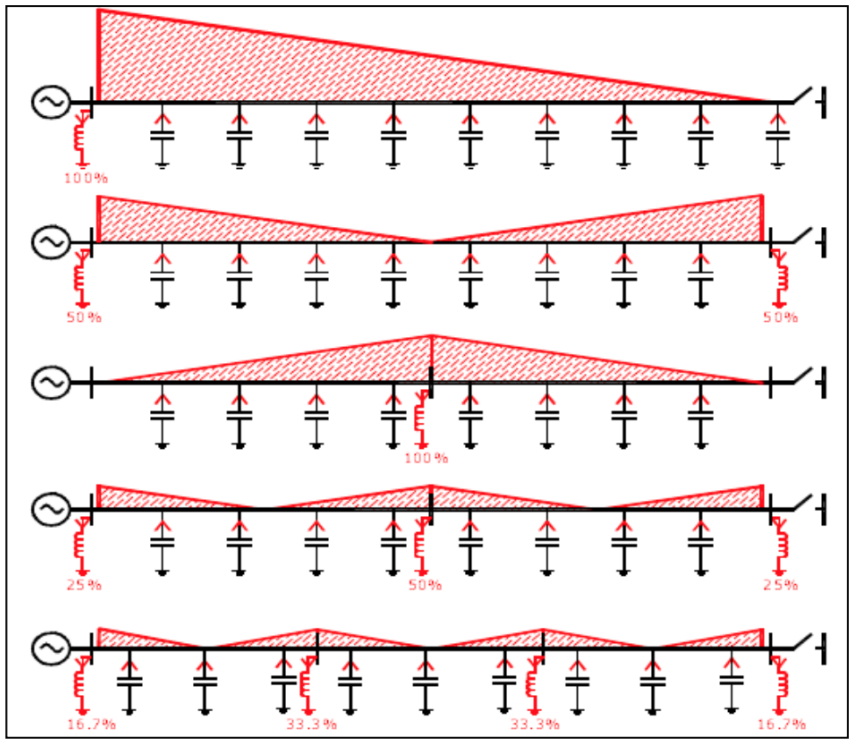

Figure A.2: Capacitive charging current depending on the placement and level of compensation [39].

Appendix B

Model

B.1 NOWITECH

The Norwegian Research Center for Offshore Wind Technology (NOWITECH) is a mulitdiscipline research program which started in 2009 by SINTEF. Through pre-competitive research the program aims to lay the foundation for industrial value creation and cost-effective offshore wind farms [45]. The main focus is challenges within large scale wind power systems on "deep-sea" (+30 m) including both bottom-fixed and floating wind turbines.

B.1.1 The Reference Turbine

It is often hard to find good information about relevant wind turbine cases without writing a confidentiality agreement with the manufacturer [46]. The NOWITECH program has therefore designed a reference turbine which can be openly shared and allows work on a common wind turbine case.

The wind turbine has a hub height above sea level of 93.5 m, and the rotor has a diameter of 141 m. The generator used in the turbine is a PMSG designed to deliver 10 MW. The wind turbine is designed for wind speed of 13 m/s and its maximum rotational speed is 13.54 rpm. The nominal line-to-line voltage of the stator is 4 kV_{rms}. The wind turbines used in this project are based on this reference turbine, but in order to make it suitable for the scope of this project some parameters has been changed. In Table B.1 some of the parameters for the reference turbine and the generator are listed [47].

Table B.1: Parameters for the NOWITECH 10 MW direct-drive PMSG.

	Symbol		Unit
Nominal Power output	P	10	MW
Design wind speed	V_{design}	13	m/s
Variable speed	n	5.5 -13.54	rpm
Optimum tip speed ratio	TSR_{opt}	7.8	-
Rotor diameter	D	141	m
Hub height	h	93.5	m
Stator nominal voltage	U_n	4 (line-line, rms)	kV
Phase resistance	R	0.0366	Ω
Phase inductance	L_a	5.29	mH
Flux linkage	λ_f	4.47	Wb

B.2 Wind Speeds

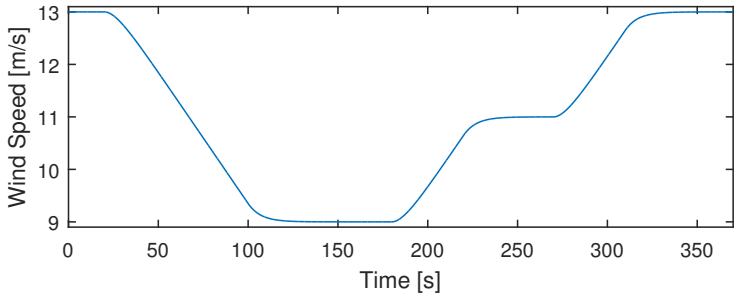

Figure B.1: The main wind speed reference used in the simulation in Section 6.1 and referred to as the main case.

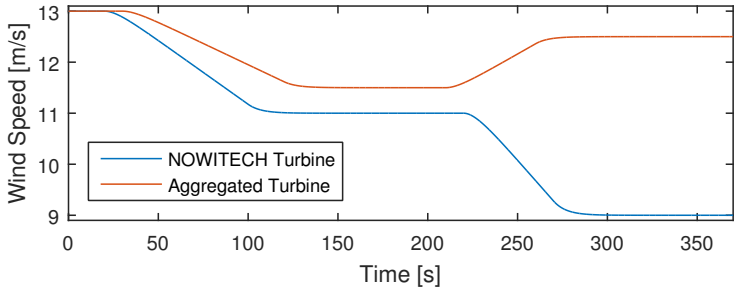

Figure B.2: The wind speeds used in the simulation in Section 6.1.3.

B.3 SimPowerSystems Model

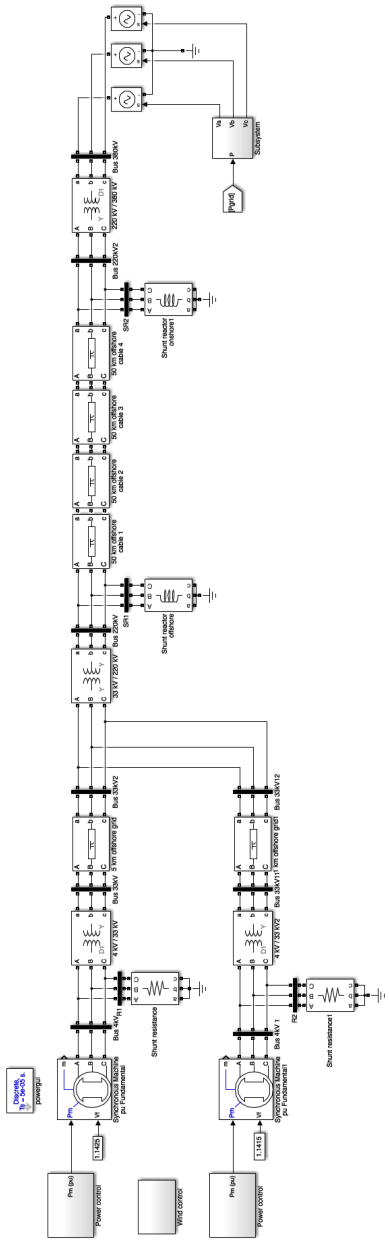

Figure B.3: The full model in SimPowerSystems.

```
%%%%%%%%%%%%%%%%%%%%%%%%%%%%%%%%%%%%%%%%%%%%%%%%%%%%%%%%%%%%%%%%%%%%%%%
%%%%%%%%%%%%%%%%%%   Final model parameters     %%%%%%%%%%%%%%%%%%
%%%%%%%%%%%%%%%%%%%%%%%%%%%%%%%%%%%%%%%%%%%%%%%%%%%%%%%%%%%%%%%%%%%%%%%

%Offshore AC grid cables
fo_spec = 50/3; % Hz
Ro = 0.2246e-3; % ohm/km
Lo = 0.43e-3; % H/km
Co = 0.18e-6; % F/km

%Transmission cable
f_spec = 50/3; % Hz,Frequency used for rlc specification

Rc = 0.1244e-3; % ohm/km
Lc = 0.43e-3; % H/km
Cc = 0.14e-6; % F/km

l_section = 50;% km

%%%%%%%%%%%%%%%%%%%%%%%%%%%%%%%%%%%%%%%%%%%%%%%%%%%%%%%%%%%%%%%%%%%%%%%
%%%%%%%%%%%%%%%%%%%%%%       fp-curve        %%%%%%%%%%%%%%%%%%%%%%
%%%%%%%%%%%%%%%%%%%%%%%%%%%%%%%%%%%%%%%%%%%%%%%%%%%%%%%%%%%%%%%%%%%%%%%

steps = 500;
margin = 10;

a = 14.399813;
b = 0.3333;
c = -0.8863;

format long;
x=linspace(0,1,steps);

y = a*x.^b+c;
speed_table_rpm = zeros(steps+margin,1);

for i=1:steps
    speed_table_rpm(i,1) = y(i);
end

for i=1:margin
    speed_table_rpm(steps+i,1) = 13.513513;
end
```

Figure B.4: The MATLAB script that follows the model.

Appendix C

Additional Results

C.1 Variable Frequency

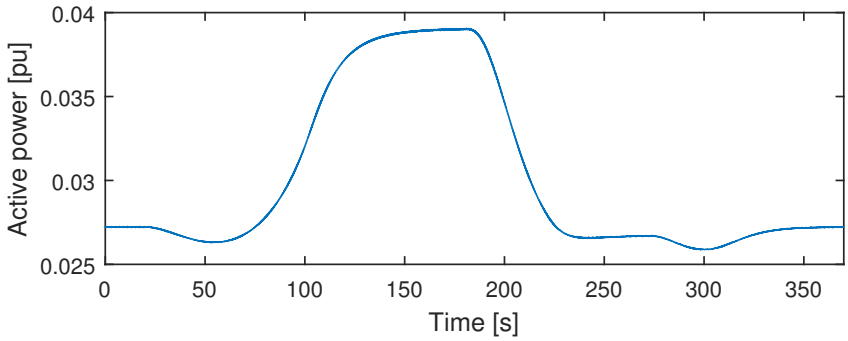

Figure C.1: Total loss from the wind turbines to the grid at a varying wind speed.

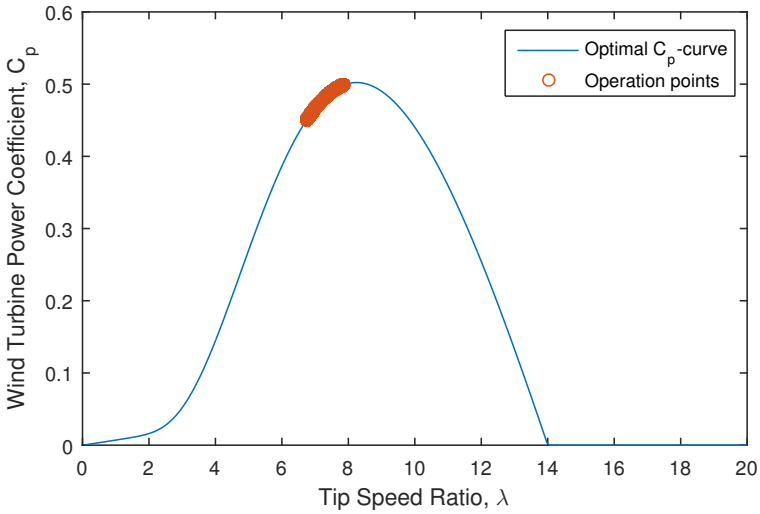

Figure C.2: Scatter plot showing the different operation points during the simulation.

C.2 Constant Frequency

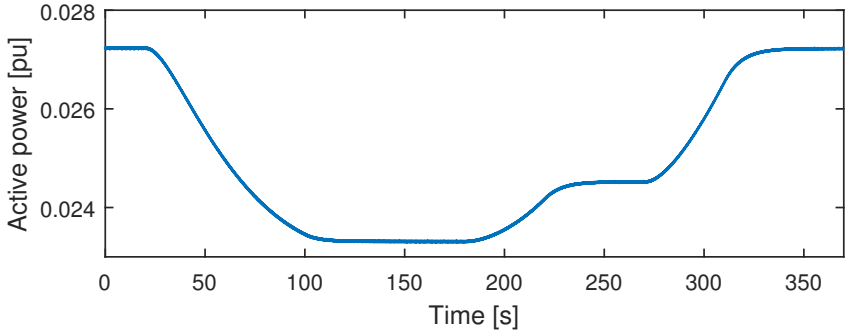

Figure C.3: Total loss from the wind turbines to the grid when the frequency is kept constant.

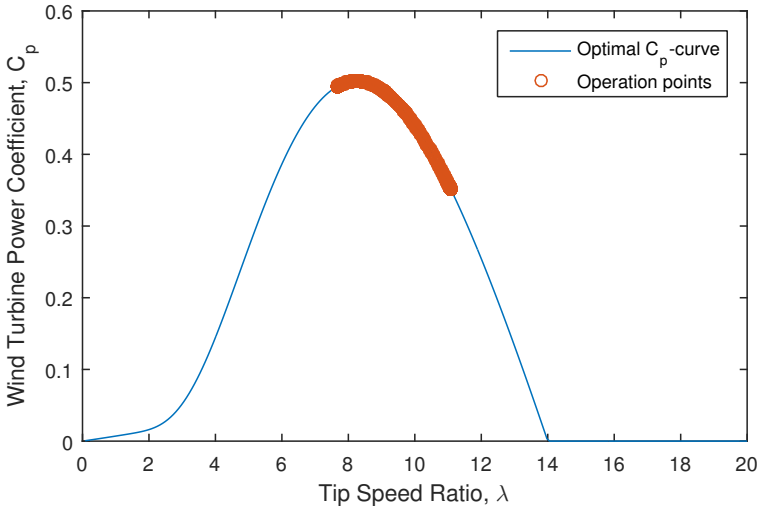

Figure C.4: Scatter plot showing the different operation points for the system when operating at a constant frequency.

C.3 Different Wind Speeds

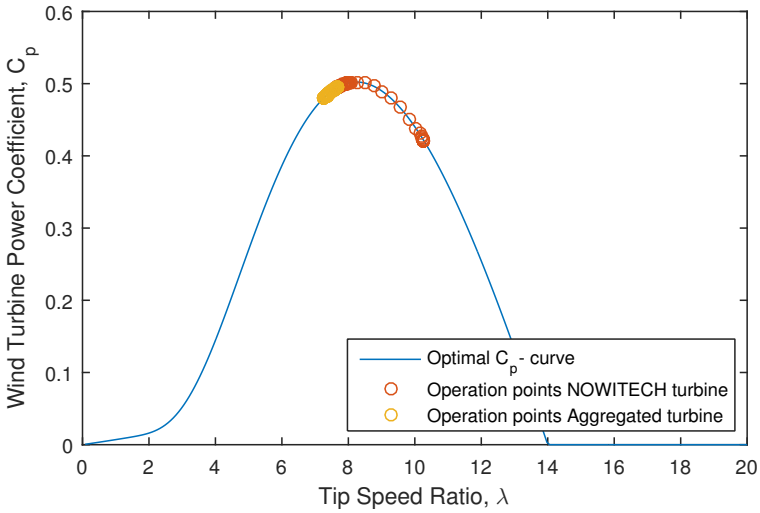

Figure C.5: Scatter plot showing the different operation points for the two turbines during the simulation with different wind speeds.

C.4 Variable Transmission Voltage

Figure C.6: Total loss from the wind turbines to the grid for the systems with different transmission voltage level at constant wind speed.

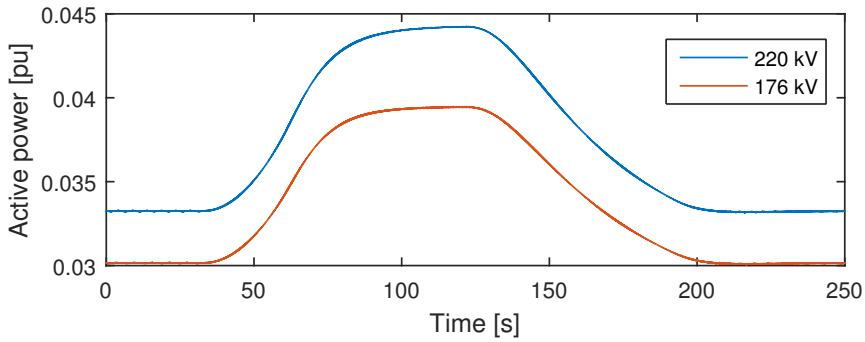

Figure C.7: Total loss from the wind turbines to the grid for the systems with different transmission voltage level at a varying wind speed.

C.5 Active Compensation

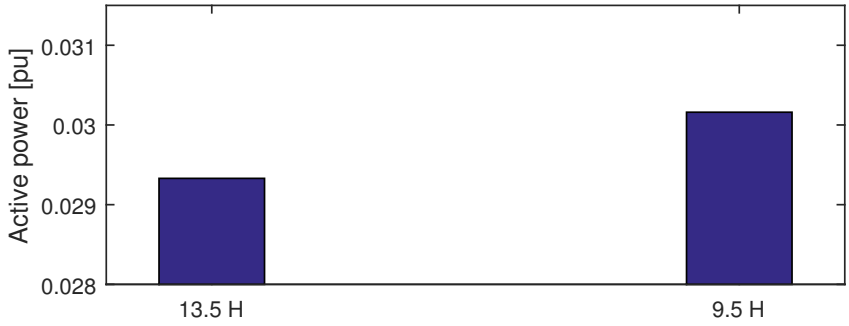

Figure C.8: Total loss from the wind turbines to the grid for the systems operating with different shunt reactors. The legend shows the inductance value used in the shunt reactors.